UPPER JURASSIC–LOWER CRETACEOUS MORRISON AND CEDAR MOUNTAIN FORMATIONS, NE UTAH–NW COLORDAO: RELATIONSHIPS BETWEEN NONMARINE DEPOSITION AND EARLY CORDILLERAN FORELAND-BASIN DEVELOPMENT

BRIAN S. CURRIE

Department of Geophysical Sciences, University of Chicago, 5734 South Ellis Avenue, Chicago, Illinois 60637, U.S.A.

ABSTRACT: **Sedimentologic, stratigraphic, and petrologic analysis of the Upper Jurassic–Lower Cretaceous Morrison and Cedar Mountain formations of Utah and Colorado provides information on the timing and nature of early Cordilleran foreland-basin development. The Morrison Formation can be subdivided into three depositional facies assemblages: (1) lower progradational shallow marine, lacustrine, fluvial, and eolian facies deposited during Oxfordian–Kimmeridgian retreat of the Stump–Sundance sea; (2) a middle assemblage containing sandy–gravelly braided fluvial deposits, which are overlain by meandering fluvial channel and overbank facies; and (3) an upper assemblage of laterally stable, low-sinuosity, fluvial channel facies deposited during Tithonian–early Neocomian (?) time. The upper part of this assemblage shows evidence of alteration and early diagenesis related to development of an Early Cretaceous unconformity. The overlying Cedar Mountain Formation is subdivided into two facies assemblages: (1) the Neocomian Buckhorn Conglomerate was deposited by northeast-trending, sandy–gravelly braided rivers that were incised into the underlying Morrison Formation; (2) an upper assemblage containing laterally stable, low-sinuosity, fluvial channel facies deposited during late Neocomian–Albian time. The base of the unit contains a thick calcrete zone that formed during an unconformity following Buckhorn deposition.**

Morrison and Cedar Mountain formation sandstones contain three petrofacies: a feldspar-rich lower Morrison petrofacies (%QmFLt = 70, 19, 11), and chert-rich upper Morrison and Buckhorn/Cedar Mountain petrofacies (%QmFLt = 54, 5, 41 and 69, 4, 27, respectively). Sandstone composition and paleocurrent data indicate a Cordilleran source area composed of Proterozoic, Paleozoic, and Mesozoic sedimentary rocks.

The Morrison Formation and Buckhorn Conglomerate were deposited in the back-bulge depozone of the Late Jurassic Cordilleran foreland-basin system and onlapped a flexural forebulge located in central Utah. Late Neocomian eastward migration of the forebulge uplifted areas in eastern Utah, producing an unconformity, while the foredeep in central Utah underwent flexural subsidence. The upper part of the Cedar Mountain Formation represents overfilling of the foredeep and deposition above the forebulge.

INTRODUCTION

The timing of initial Cordilleran foreland-basin development in the western interior United States has been the subject of considerable debate. Earlier workers suggested that thrusting in the Sevier thrust belt of Utah, Wyoming, and Idaho commenced during regional deposition of nonmarine Upper Jurassic rocks (Armstrong and Cressman 1963; Suttner 1969; Furer 1970; Young 1970; Jordan 1981; Wiltschko and Dorr 1983). More recent investigations have concluded that the onset of thrust-related crustal loading and asymmetric foreland-basin subsidence occurred earlier and is represented by deposition of the Middle–Late Jurassic Twin Creek, Pruess, and Stump formations and their correlatives in Utah, southern Idaho, and western Wyoming (Thorman et al. 1992; Bjerrum and Dorsey 1995). Structural and metamorphic studies in eastern Nevada and western Utah document contractional deformation, magmatism, and regional metamorphism that supports a Middle Jurassic age for crustal shortening (Hudec 1992; Miller 1992; Snoke et al. 1992; Wells 1992). DeCelles and Burden (1992) proposed that the Upper Jurassic nonmarine deposits across the foreland represent the late-stage filling of the Middle Jurassic Cordilleran foreland basin, and were derived from thrusts found today in the hinterland of the Sevier belt.

In contrast, Heller et al. (1986), Heller and Paola (1989), and Yingling and Heller (1992) suggested that Late Jurassic deposition pre-dated Sevier deformation. This interpretation is based primarily on the observation that the first observable thickening of stratigraphic units towards the Sevier thrust belt in Utah occurs in the Lower Cretaceous Cedar Mountain Formation and correlative units. Lawton (1994) supported this interpretation and indicated that Middle–Upper Jurassic rocks in the western interior were deposited during a period of subduction-related subsidence prior to deformation in the Sevier belt.

Contributing to the lack of understanding of early Cordilleran foreland-basin development is the limited number of regionally integrated sedimentologic, stratigraphic, and provenance investigations of the Jurassic–Cretaceous nonmarine interval. The goal of this paper is to document the Upper Jurassic–Lower Cretaceous Morrison and Cedar Mountain formations in northeastern Utah and northwestern Colorado and to demonstrate that these deposits record early Cordilleran foreland-basin development. Sedimentologic, petrologic, and geochronologic data from these formations are used to determine the age, deposystems, provenance, and paleogeography of these rocks, and to establish a regional correlation with equivalent units in central Utah.

Stratigraphy and Age

In the area surrounding the eastern Uinta Mountains region (Fig. 1) the Morrison Formation consists of four lithostratigraphic members: The Windy Hill, Tidwell, Salt Wash, and Brushy Basin members (Fig. 2) (Turner 1992). These members can be identified at most locations in the study area, although thicknesses and facies vary (Fig. 3). The Morrison Formation overlies marine sandstone, limestone, and shale of the Oxfordian Redwater Member of the Stump Formation (Pipiringos and O'Sullivan 1978). The Morrison is overlain by the Cedar Mountain Formation, which consists of the lower Buckhorn Conglomerate Member and an upper unnamed mudstone/sandstone member (Stokes 1952; Kirkwood 1976). The Buckhorn Conglomerate Member is restricted to the southern and northeastern parts of the study area (Fig. 3). Where the conglomerate is absent, upper Cedar Mountain mudstone lies directly on Brushy Basin Member mudstone. At these locations, the base of the Cedar Mountain Formation is defined by the first occurrence of large (> 10 cm diameter), coalesced carbonate nodules or a laminar to structureless calcrete lying above the Brushy Basin Member. The top of the Cedar Mountain Formation is defined by an unconformable contact with the overlying fluvial sandstones of the Albian–Cenomanian Dakota Formation (Vaughn and Picard 1976; Molenaar and Cobban 1991; Currie et al. 1993).

The geochronologic data summarized in Table 1 show that the Morrison and Cedar Mountain formations were deposited between Oxfordian (Late Jurassic) and Albian (Early Cretaceous) time. Data from the Morrison Formation indicate Oxfordian through Tithonian deposition, although deposition of the upper parts of the formation may have extended into Early Cretaceous time. $^{40}Ar/^{39}Ar$ dating of a bentonite in Tidwell Member near the 1IP section (Fig. 3) has yielded an Oxfordian–Kimmeridgian age of

JOURNAL OF SEDIMENTARY RESEARCH, VOL. 68, NO. 4, JULY, 1998, P. 632–652

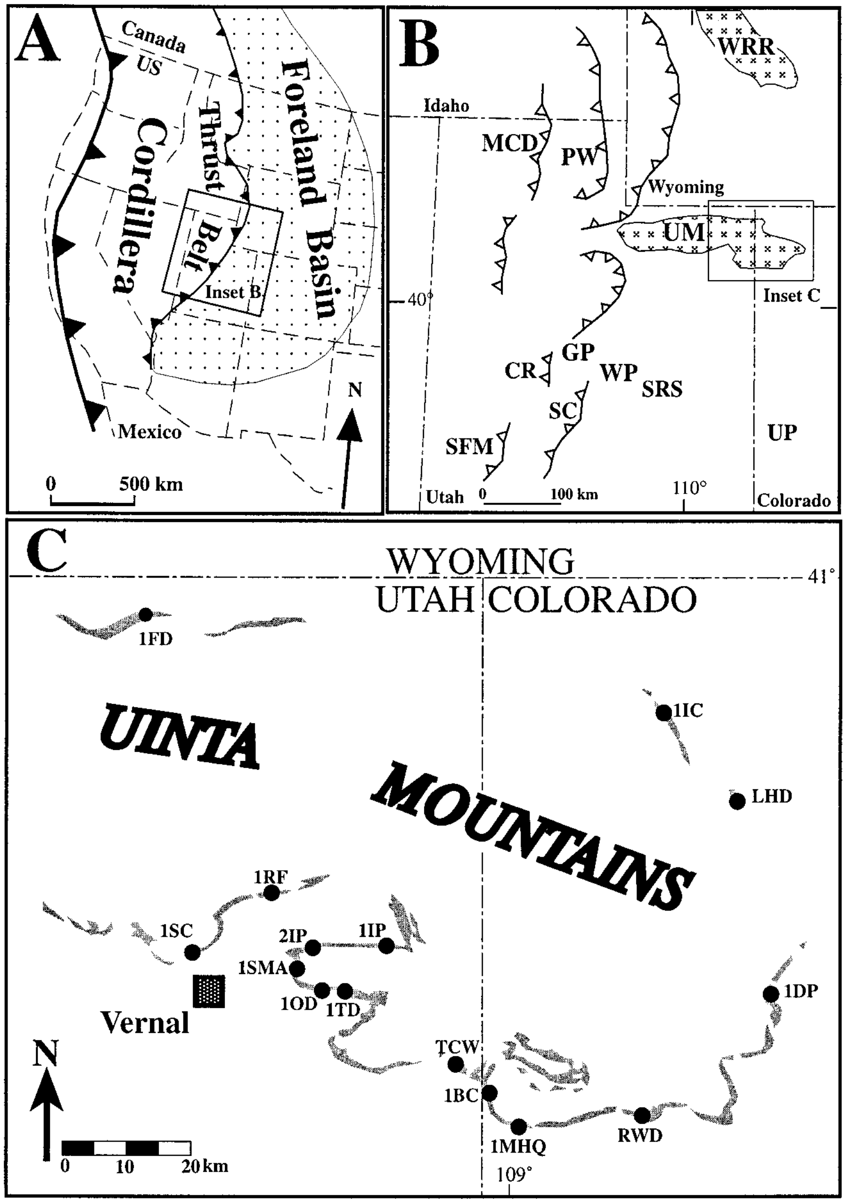

FIG. 1.—**A)** Generalized map showing tectonic setting of the Cordilleran foreland basin. Heavy barbed line shows approximate location of the Jurassic–Cretaceous subduction zone; light barbed line represents final location of the leading edge of the Cordilleran fold and thrust belt. After Dickinson and Snyder (1978). **B)** Generalized map of the south-central part of the foreland basin showing location of the study area (Inset C), nearby Laramide uplifts, individual segments of the thrust belt, and locations mentioned in the text. Abbreviations are as follows: WRM, Wind River Mountains; UM, Uinta Mountains; SRS, San Rafael Swell; UP, Uncompahgre Plateau; GP, Gunnison Plateau; WP, Wasatch Plateau; SC, Salina Canyon; CR, Canyon Range thrust sheet; SFM, San Francisco Mountains; PW, Paris–Willard thrust; MCD, Manning Canyon detachment. **C)** Map of the study area showing outcrops of Jurassic–Cretaceous nonmarine rocks (shaded areas) and measured sections referred to in the text (dark circles). Outcrop locations are listed in Appendix 1.

154.8 ± 0.6 Ma (Kowallis et al. 1998), based on the time scale of Gradstein et al. (1995). The Salt Wash Member at the 1IP section has yielded Tithonian palynomorphs near the top of the member (H.T. Pile, personal communication 1992). $^{40}Ar/^{39}Ar$ dating of a bentonite from the middle Brushy Basin Member near the 1TD section (Fig. 3) has also yielded a Tithonian age (149.0 ± 0.4 Ma) (Kowallis et al. 1998). K/Ar dating of biotite from a bentonite from the upper part of the Brushy Basin Member near the 1TD section yielded an Early Cretaceous age of 135.2 ± 5.5 Ma (S.A. Bilbey, personal communication 1993). However, $^{40}Ar/^{39}Ar$ dates from the same horizon yielded a Jurassic age of 152.9 ± 1.2 Ma (Kowallis et al. 1991). This discrepancy leaves the age of the upper 25–40 m of the Morrison Formation in question. The Late Jurassic age of the Tidwell–middle Brushy Basin members is corroborated by chronostratigraphic evidence from throughout the region (Table 1).

The age of the Cedar Mountain Formation in the study area is poorly constrained. The only age-diagnostic fossils were reported by Hansen (1965), who noted Aptian/Albian charophytes and ostracodes in the upper Cedar Mountain Formation on the north flank of the Uinta Mountains (1FD section, Fig. 3). However, geochronologic data from the Cedar Mountain Formation in other parts of Utah and Colorado indicate a Barremian–Albian age of deposition (Table 1).

Given the Oxfordian–Early Neocomian (?) age of the underlying Morrison Formation and the Barremian–Albian age of the overlying upper Cedar Mountain Formation, the Buckhorn Conglomerate is considered to be mid-Neocomian in age (Fig. 2).

SEDIMENTOLOGY

The Morrison and Cedar Mountain formations in northeastern Utah and northwestern Colorado consist of up to 275 m of mudstone, sandstone, conglomerate, and minor limestone. The main characteristics of the stratigraphic members (Fig. 2) are briefly described in Table 2 and interpreted below.

Morrison Formation

Windy Hill Member.—The Windy Hill Member in the study area consists of 0.5–3 m of very fine- to medium-grained sandstone. On the basis

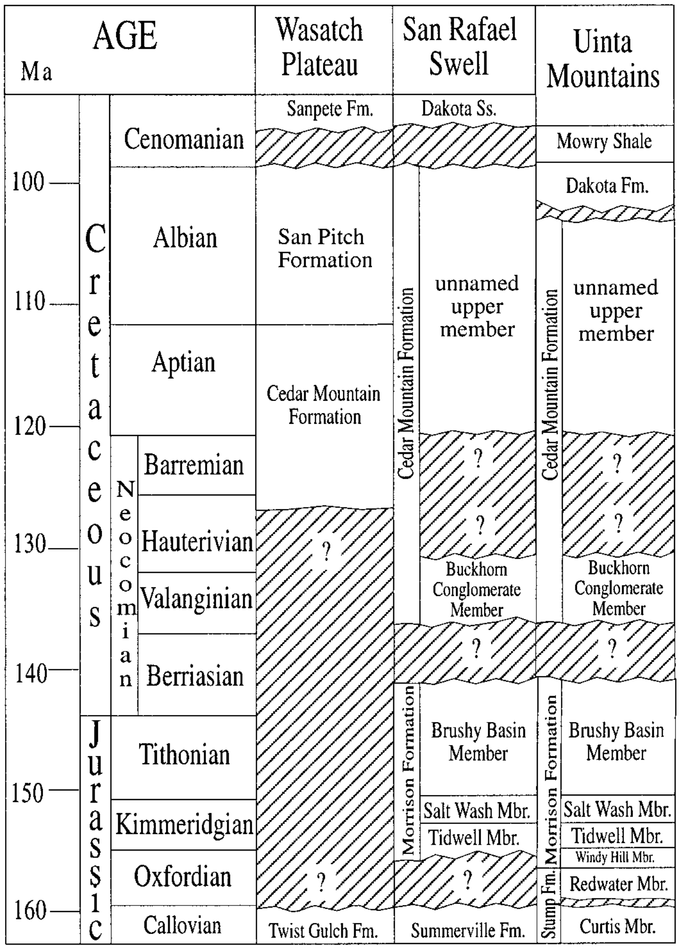

FIG. 2.—General stratigraphic nomenclature of the Jurassic–Cretaceous nonmarine rocks of central–northeast Utah and northwest Colorado. Formation ages are based on chronostratigraphic data discussed in the text. Time scale is from Gradstein et al. (1995).

of the lithofacies described in Table 2, the Windy Hill Member is interpreted as shallow marine and foreshore deposits. The low-angle to horizontal lamination with primary current lineations is characteristic of foreshore deposits (Clifton 1969), whereas the small-scale trough cross-stratification represents sand deposition by longshore currents or in shallow channels that incised the upper shoreface (e.g., Hunter et al. 1979). Symmetrical ripples in the Windy Hill formed by oscillatory, wave-driven currents in lower shoreface or shallow marine environments.

Tidwell Member.—The Tidwell Member consists of 3–14 m of interbedded sandstone and mudstone (Table 2). The Tidwell Member in the study area is interpreted as the deposits of a marginal marine, tidal/estuary complex. The tabular sandstone bodies containing symmetrical ripples are interpreted as tidal-sand-flat deposits that were subjected to oscillatory, wave-driven currents (Weimer et al. 1982). The lenticular sandstone bodies containing trough and ripple cross-stratification and flaser bedding are indicate deposition in tidal channels or tidally influenced fluvial channels (Reineck and Wunderlich 1968). Structureless to laminated and fissile mudstones with symmetrical ripple cross-lamination and wavy bedding are interpreted as lagoon or tidal-flat deposits (Ward and Ashley 1989; Ginsburg 1975). The presence of desiccation cracks in some of the mudstone beds is an indication of subaerial exposure on tidal flats or in overbank environments.

Salt Wash Member.—The Salt Wash Member in the study area can be subdivided into two genetically related units: a lower sandstone/mudstone, and an upper sandstone/conglomerate. The lower part of the Salt Wash Member consists of 9–65 m of interbedded sandstone, mudstone, and limestone (Fig. 3, Table 2). Coalesced sandstone lenses of the lower Salt Wash are interpreted as the deposits of a sandy, fluvial channel system. The laterally continuous nature of the sandstone bodies suggests deposition in unstable, interconnected channels. The lack of lateral accretion surfaces and levee deposits suggests that the fluvial system was braided.

The massive, mottled and bioturbated mudstone containing nodular carbonate is interpreted as overbank deposits that were subject to pedogenic modification and paleosol formation. The dark gray and green fissile shale and silty limestone are interpreted as the deposits of shallow ponds and lakes on the floodplain.

The thick, fine- to medium-grained sandstone containing giant planar-tangential cross-strata is interpreted as eolian deposits (TCW and 1DP sections, Fig. 3). These represent eolian dune slip faces that migrated under

TABLE 1.—*Late Jurassic–Early Cretaceous geochronologic data.*

Formation/Member	Level/Section	Data Type	Age (Ma)	Age	Source
Study Area Data					
Morrison Fm.					
Tidwell Member	~7.5 m, 1IP	Ar/Ar	154.8 ± 0.6	Oxfordian-Kimmeridgian	2
upper Salt Wash Member	87.5 m, 1IP	palynomorphs	—	Tithonian	6
middle Brushy Basin Member	~175 m, 1TD	Ar/Ar	149.0 ± 0.4	Tithonian	2
upper Brushy Basin Member	~200 m, 1TD	K/Ar, Ar/Ar	152.9 ± 1.2, 135.2 ± 5.5	Kimmeridgian, Berriasian	1, 5
Cedar Mountain Fm.					
upper Cedar Mountain Fm.	middle (?), 1 FD	charophytes/ostracodes	—	Aptian/Albian	8
Regional Data					
Morrison Fm.					
Tidwell Member	base, NE Circle Cliffs Uplift	Ar/Ar	154.8 ± 0.6	Oxfordian–Kimmeridgian	2
middle Brushy Basin Member	base-top, NE San Rafael Swell	Ar/Ar	150.2 ± 0.5, 148.1 ± 0.5	Tithonian	2
middle Brushy Basin Member	base-top, SE Utah	Ar/Ar	149.4 ± 0.7, 147.6 ± 0.8	Tithonian	1
Lower Cretaceous					
Burrow Canyon Fm.	middle, Western Colorado	palynomorphs	—	Barremian-Early Albian	4
upper Cedar Mountain Fm.	?, central Utah	molluscs	—	Aptian/Albian	9
upper Cedar Mountain Fm.	?, central Utah	plant macrofossils	—	Aptian/Albian	10
upper Cedar Mountain Fm.	lower, Eastern Utah	vertebrates	—	Barremian	11
upper Cedar Mountain Fm.	top, SW San Rafael Swell	palynomorphs	—	Late Albian	4
upper Cedar Mountain Fm.	top, SW San Rafael Swell	Ar/Ar	98.39 ± 0.07	Late Albian	7

Sources: 1. Kowallis et al. (1991); 2. Kowallis et al. (1998); 3. Peterson (1992); 4. Tschudy et al. (1984); 5. S.A. Bilbey, personal communication (1993); 6. H.T. Pile, personal communication (1992); 7. Cifelli et al. (1997); 8. Hansen (1965); 9. Katich (1951), Stokes (1952); 10. Simmons (1957), Thayn (1973); 11. Kirkland (1992).

prevailing west–southwesterly winds. The inversely graded, parallel lamination is interpreted as subcritically climbing translatent strata, deposited on dune surfaces by migrating eolian ripples (e.g., Hunter 1977).

The upper part of the Salt Wash Member is characterized by 12–40 m of sandstone, chert granule–pebble conglomerate, and minor amounts of mudstone (Table 2, Fig. 4A). As a whole, the maximum grain size in the unit coarsens upsection from coarse sand at the base to pebble-size clasts at the top.

The upper Salt Wash Member is interpreted as the deposits of a sandy–gravelly braided fluvial system. Laterally continuous sandstone and conglomerate bodies were deposited by laterally unstable, interconnected channels. Individual lenses of trough cross-stratified sandstone and conglomerate were deposited as sandy–gravelly macroforms that migrated downstream during high-flow events. Paleocurrent data from planar and trough cross-stratification in the sandstones and conglomerates indicate east-southeastward paleoflow, with a minor component of flow toward the northeast and southwest (Fig 4A). Mudstone interbeds containing carbonate nodules represent overbank deposits modified by pedogenic processes. The increased grain size at the top of the unit indicates progradation of coarser facies in the direction of transport through time.

Brushy Basin Member.—The Brushy Basin Member can be subdivided into lower, middle, and upper units. The lower part of the Brushy Basin Member consists of 20–45 m of sandstone and mudstone (Fig. 3, Table 2, Fig. 4B). Sandstone bodies in the lower part of the Brushy Basin Member are interpreted as deposits of fluvial channels with variable sinuosity. The increasing lateral discontinuity, and the presence of lateral accretion surfaces in the channel sandstones in the upper part of the unit, indicate a transition from braided to meandering fluvial morphologies. Mottled mudstones containing root traces, cutans, peds, and abundant carbonate nodules are interpreted as well-developed calcic-paleosol horizons.

The middle part of the Brushy Basin Member consists of 44–68 m of mudstone, sandstone, conglomerate, and limestone (Table 2, Figs. 3, 4B). The middle Brushy Basin Member is interpreted as the deposits of a poorly drained, mud-dominated, alluvial/lacustrine plain. The dark color of the mudstones is attributed to reducing conditions that developed in response to a high ground-water table. The smectitic nature of the mudstone and the presence of abundant bentonite beds indicate a probable volcanic source for much of the sediment. Laminated mudstones and thin-bedded limestones and siltstones are interpreted as shallow lacustrine or pond deposits. The massive mudstone containing root traces and nodular carbonate zones represents overbank or ephemeral lacustrine deposition that was later subject to pedogenic processes. The bentonite beds in the unit are interpreted as volcanic ashes that were deposited by air fall on the alluvial plain or in shallow lacustrine settings. The presence of rounded quartz grains in some of these ash beds suggests partial reworking and contamination by fluvial and/or eolian processes. Desiccation cracks and gypsum crystals in the unit indicate episodic drying of the flood plain as well as the possibility of the existence of evaporitic conditions in ephemeral lakes and ponds. This indicates that the middle Brushy Basin Member may have been deposited in a semiarid to seasonally arid climate. The presence of a semiarid climate during middle Brushy Basin Member deposition is corroborated by Turner and Fishman (1991), who documented an alkaline/saline lake deposit in the Brushy Basin Member of the east-central Colorado Plateau.

The sandstone bodies in the middle Brushy Basin Member are interpreted as deposits of eastward-flowing fluvial channels of moderate sinuosity. The large bodies of coarse-grained sandstone are interpreted to be major fluvial channels, whereas the thinner beds of finer-grained sandstone represent small tributaries or secondary channels that were active only during floods (e.g., Rust 1981; Schumann 1989). The low width/thickness ratios of the channels and the lack of lateral-accretion surfaces indicate that the primary mode of channel migration was by avulsion. Paleocurrent data from planar and trough cross-stratification in the sandstones and conglomerates indicate northeastward to southeastward transport directions (Fig. 5B, Fig. 3). Some of the thin, rippled sandstone and siltstone beds in the unit may have been deposited on the floodplain as crevasse-splay sheets (e.g., Smith and Pérez-Arlucea 1994).

A possible modern analog for middle Brushy Basin Member deposition is the Cooper's Creek fluvial/alluvial system in the Lake Eyre Basin of central Australia (Bell 1986), wherein low- to moderate-sinuosity, anastomosing fluvial channels supply sediment for a mud-dominated alluvial plain (Rust 1981). The Cooper's Creek system is also similar to the middle Brushy Basin Member in that deposition occurs in a semiarid climate and is associated with a downstream alkaline/saline lacustrine system (Turner and Fishman 1991).

The upper part of the Brushy Basin Member contains 25–45 m of mudstone, sandstone, and conglomerate (Table 2, Fig. 4C). The unit is present throughout the study area, although it is thinned or absent where the Buckhorn Conglomerate is present (Fig. 3). Chert grains and clasts in the upper part of the Brushy Basin Member have dark interiors that are surrounded by white, diagenetic reaction rims. In addition, many of the altered chert clasts and grains exhibit pitted surfaces and porous interiors that may be related to partial diagenetic dissolution. The dark-colored interiors of altered chert pebbles are similar to those in unaltered conglomerates of the middle Brushy Basin Member.

The upper part of the Brushy Basin Member is interpreted as deposits of a low-sinuosity fluvial system similar to the underlying middle Brushy Basin. Lenticular conglomerate and sandstone bodies were deposited by stable fluvial channels, whereas horizontally laminated and asymmetrically rippled siltstone and sandstone beds present laterally from the channel bodies are interpreted as levee or crevasse-splay deposits. Paleocurrent data from trough and planar cross-stratification in the channel bodies indicate southeastward paleoflow (Fig. 5B).

The distinct color banding in the mudstones of the upper unit is interpreted to be the result of leaching of upper soil horizons by meteoric waters (Fig. 4C; Shanmugam 1988). The bleaching and partial dissolution of coarser-grained units may indicate leaching by migration of groundwater through porous channel sediments (Shanmugam and Higgins 1988). The siliceous nature of upper Brushy Basin mudstones and the rarity of nodular carbonate within this interval suggest that sediment alteration may be related to increased precipitation during or after deposition (Shanmugam 1988; Mack 1992). Early diagenesis by pedogenic and groundwater processes may also be an indication of long periods of little or no deposition and subsequent paleosol formation and alteration of upper Brushy Basin sediments. As such, alteration of this interval may have occurred during development of the regional Late Jurassic–Early Cretaceous ''K'' unconformity described by Pipiringos and O'Sullivan (1978).

Cedar Mountain Formation

Buckhorn Conglomerate Member.—The Buckhorn Conglomerate Member of the Cedar Mountain Formation consists of 1–35 m of conglomerate, sandstone, and minor mudstone (Fig. 3, Table 2). Overall, the unit fines upward from pebble and cobble conglomerate at the base to medium- and fine-grained sandstone at the top. The Buckhorn Conglomerate is present in an east–west-striking, 25 km wide outcrop belt across the southern part of the study area, and in one small outcrop along the northeastern margin of the study area (Fig. 3, Fig. 5C). The thickness of the Buckhorn Member progressively decreases from 35 m near Dinosaur, Colorado to nearly zero in the vicinity of Cliff Creek, Utah, and Skull Creek, Colorado. Conglomerate and very coarse sandstone of the Buckhorn rest in erosional contact upon greenish-gray mudstone and fine-grained sandstone of the middle and upper Brushy Basin Member of the Morrison Formation (Fig. 6B). Conglomerate clasts are dominated by gray, black, and brown chert with minor amounts of white chert and quartzite (Fig. 6C). Average maximum conglomerate clast sizes generally decrease from 9.3 cm at the base of the unit to 1.5 cm at the top.

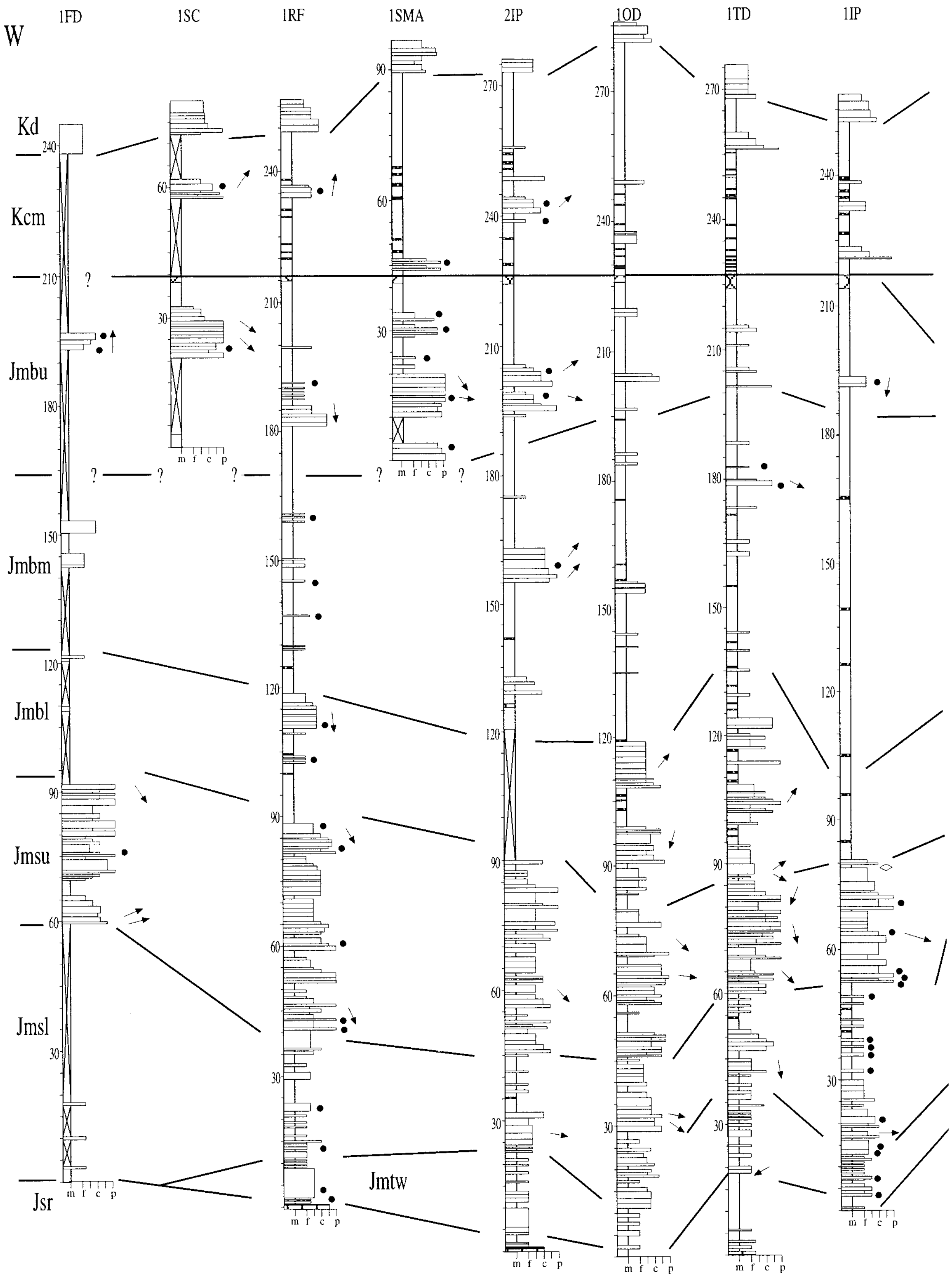

FIG. 3.—Logs of measured stratigraphic sections and correlations of the Morrison and Cedar Mountain formations, NE Utah–NW Colorado. Section locations are shown in Figure 1 and listed in Appendix 1.

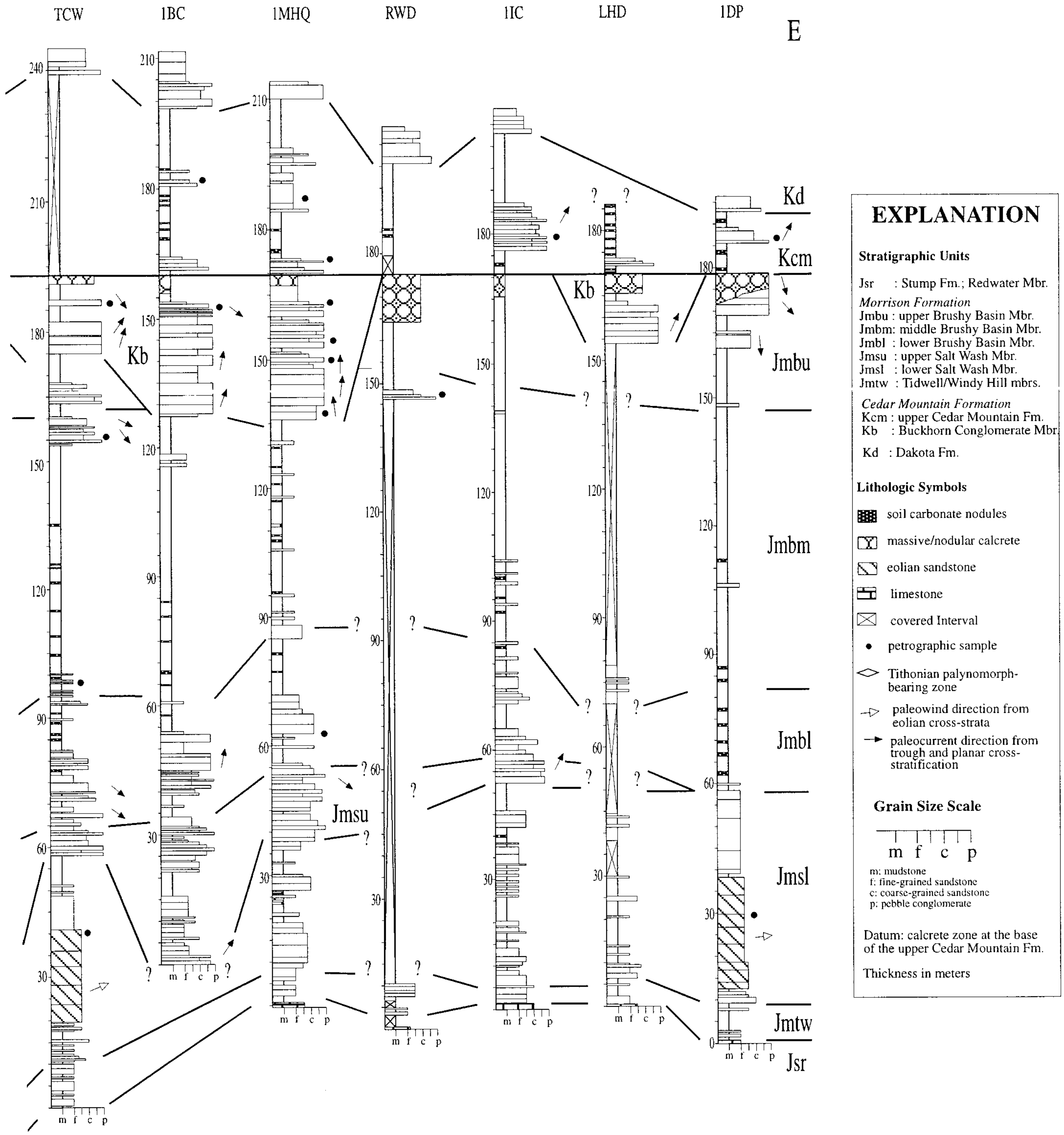

FIG. 3.—Continued.

The coarse grain size, predominance of clast-supported conglomerate, abundance of trough and planar cross-stratification, and laterally continuous nature of the conglomerate bodies indicate that the Buckhorn Conglomerate was deposited in laterally unstable, interconnected, gravelly braided fluvial channels (e.g., Williams and Rust 1969; Miall 1977; Rust 1978). The coalesced lenticular conglomerate bodies represent gravelly, high-flow-stage macroforms, whereas the thin lenses of interbedded sandstone were deposited by migration of sandy bedforms during waning and post-flood stages of flow (e.g., Rust 1972; Ramos and Sopeña 1983). Paleocurrent data from trough and planar cross-stratification in both the conglomerate and interbedded sandstone indicate a north-northeastward direction of paleoflow (Fig. 5C; Fig. 3). Mudstones in the Buckhorn are interpreted as overbank deposits that were disrupted and homogenized by pedogenic processes.

Paleocurrent and isopach data indicate that the Buckhorn Conglomerate

TABLE 2.—*Lithologic and sedimentologic characteristics, Morrison and Cedar Mountain formations.*

Formation/ Member	Thickness	Geometry, Bedding, Lithology	Sedimentary Structures	Paleo-current Orienta-tions	Fossils	Interpretation
Morrison Fm.						
Windy Hill Mbr.	0.5–3 m	tabular, very fine- to medium-grained, thin- to thick-bedded, light gray to white sandstone	low-angle planar/horizontal lamination, primary current lineations, symmetrical, straight-crested ripples, small-scale trough cross-stratification		marine bivalve *Ostrea*	shallow marine, foreshore
Tidwell Mbr.	3–14 m	tabular, very fine- to medium-grained, medium to thick bedded, tan to white sandstone	symmetrical, sinuous-, straight-crested ripples			tidal sand flat
		lenticular, very fine- to medium-grained, medium to thick bedded, tan to white sandstone	small-scale, ripple- and trough cross-lamination, ripple reactivation surfaces			tidal/estuary channel
		tabular, structureless to thinly laminated, locally fissile, thin- to very thick-bedded mudstone	symmetrical ripples, wavy bedding, mudcracks			tidal flat, lagoon
Salt Wash Mbr. (lower)	9–65 m	laterally continuous, coalesced lenses of thick- to very thick-bedded, upward-fining, coarse- to very fine-grained, white-tan sandstone with abundant mud ripup clasts	trough and ripple cross-stratification, horizontal lamination	E–SE		sandy, braided fluvial channels
		gray, green, red, medium- to very thick-bedded mudstone with abundant calcareous nodules	structureless to mottled, common root traces			alluvial plain
		dark gray to green, medium- to thick-bedded fissile shale, interbedded gray, silty micritic limestone			nonmarine charophytes and molluscs (Schudack et al. 1998)	shallow lakes/ponds
		fine- to medium-grained, well sorted, very thick-bedded, white to reddish-gray sandstone	Giant (up to 8 m thick), planar-tangential cross-stratification with abundant thin parallel, inversely graded lamination	E–NE		eolian dunes
Salt Wash Mbr. (upper)	12–40 m	laterally continuous, coalesced lenses of thick- to very thick-bedded, upward-fining, tan-gray pebble/granule conglomerate and very coarse- to fine-grained sandstone	trough and planar cross-stratification, primary current lineations, small-scale asymmetrical ripple cross-lamination	E–SE		sandy/gravelly braided fluvial channels
		gray and green/red, medium- to very thick-bedded mudstone with abundant calcareous nodules	structureless to mottled, common root traces		palynomorphs	alluvial plain
Brushy Basin Mbr. (lower)	20–45 m	laterally continuous to laterally restricted, thick- to very thick-bedded, upward-fining, tan-gray pebble/granule conglomerate and very coarse- to fine-grained sandstone; sandstone bodies become more laterally restricted upsection	trough and planar cross-stratification, asymmetrical ripple cross-lamination, plane-parallel lamination, primary current lineation, ~3 m high lateral-accretion surfaces near top	NE–SE		braided to meandering fluvial channels
		red, green, and gray, medium- to very thick-bedded sandy mudstone with abundant calcareous nodules	structureless to mottled, root traces, cutans, and blocky peds			alluvial plain
Brush Basin Mbr. (middle)	44–68 m	dark green/gray, thinly laminated to massive, thick- to very thick-bedded, smectitic mudstone, nodular carbonate and gypsum (selenite) crystals present in some horizons	root traces, rare desiccation cracks	NE–SE		alluvial/lacustrine plain
		tabular to lenticular, white, greenish-yellow, red, thin- to medium-bedded, waxy bentonite containing euhedral apatite, zircon, biotite, plagioclase, and sanidine crystals and rounded quartz grains	structureless to thinly laminated			volcanic ashes deposited by air fall on the alluvial plain or in shallow lacustrine settings
		tabular to lenticular, medium- to thin-bedded siltstone and micritic limestone	structureless to symmetrical ripple cross-lamination		nonmarine gastropods, charophytes	shallow lakes/ponds
Brushy Basin Mbr. (middle)		lenticular, upward-fining, thin- to very thick-bedded, tan-gray pebble conglomerate and very coarse- to medium-grained sandstone, 2–15 m thick and up to 1 km in lateral extent	trough and planar cross-stratification, although portions appear massive to crudely horizontally stratified		abundant dinosaurs	laterally stable, low-sinuosity fluvial channels
		lenticular to tabular, thin- to medium-bedded, silty to fine-grained, gray sandstone	structureless to asymmetric ripple cross-laminated			secondary fluvial channels, crevasse splays
Brush Basin Mbr. (upper)	25–45 m	red, purple, white, yellow, gray, and green, sandy, siliceous, medium- to very thick-bedded mudstone; a distinctive red/white color banding is prevalent in the upper 15 m of the unit		NE–SE		alluvial plain

TABLE 2.—*Continued.*

Formation/ Member	Thickness	Geometry, Bedding, Lithology	Sedimentary Structures	Paleo-current Orienta-tions	Fossils	Interpretation
		lenticular, upward-fining, thin- to very thick-bedded, white-tan pebble conglomerate and very coarse- to medium-grained sandstone bodies, 3–10 m thick and up to 300 m wide.	trough and planar cross-stratification and horizontal stratification			laterally stable, low-sinuosity fluvial channels
		tabular, very fine-grained, white-tan sandstone and siltstone beds that contain sharp, nonerosive bases	horizontal lamination and asymmetrical ripple cross-lamination			
Cedar Mountain Fm.						
Buckhorn Conglomerate Mbr.	1–35 m	laterally continuous, coalesced lenses of thick- to very thick-bedded, upward-fining, gray, clast-supported conglomerate with individual clast sizes up to 12 cm in diameter and very coarse- to fine-grained sandstone	trough and planar cross-stratification, horizontal stratification, primary current lineations, small-scale asymmetrical ripple cross-lamination	N–NE		gravelly, sandy braided fluvial channels
		green, white, red, medium- to very thick-bedded sandy mudstone	mottled to structureless, rare root traces			alluvial plain
upper Cedar Mountain Fm.	15–40 m	laterally continuous, 1–10 m thick zone of large (up to 40 cm diameter) coalesced gray/purple micritic carbonate nodules, and white/gray, laminar to massive micritic carbonate	pisolites, replaced detrital grains and argillaceous material, floating pebbles, smaller, concentrically laminated, brecciated nodules, spar-filled vugs, veins of sparry calcite and silica			unconformity-related petrocalcic horizon
		green, red, and dark gray to black sandy mudstone; calareous nodules abundant in the lower ⅔ of the unit; carbonaceous in upper ⅓ of unit	structureless to mottled, common root traces			alluvial plain
		lenticular, medium- to thin-bedded, gray micritic limestone	structureless to weakly laminated		nonmarine gastropods, charophytes and ostracodes	shallow lakes/ponds
		lenticular, upward-fining, thin- to very thick-bedded, tan, very coarse- to very fine-grained sandstone bodies up to 4 m thick and 300 m wide. Sandstone bodies increase in size and abundance up-section and may be stacked vertically	trough cross-stratification, small-scale ripple cross-lamination, primary current lineations	NE		laterally stable, low-sinuosity fluvial channels

was deposited in an $\sim$ 25 km wide northeast–southwest-trending trunk fluvial system. The confined nature of conglomerate distribution, the symmetrical thinning patterns observed east and west of the trunk axis, and the absence or thinning of the upper Brushy Basin Member where the Buckhorn is present imply that the Buckhorn Member represents the filling of a valley eroded into the underlying Morrison Formation. The upward-fining nature of the coarse-grained fraction and the increase in overbank mudstone toward the top of the unit indicate an overall decrease in stream gradient during Buckhorn deposition. This change conforms with predicted fluvial gradients and sedimentation patterns associated with the latter stages of valley-fill sequences (e.g., Shanley and McCabe 1994).

Upper Cedar Mountain Formation.—The upper Cedar Mountain Formation consists of 15–40 m of interbedded sandstone, mudstone, and limestone. The unit is present throughout the study area, although it thins significantly from west to east (Fig. 3). The base of the unit is defined by the first occurrence of a 1–10 m thick, nodular to crudely laminar or structureless calcrete horizon lying on top of the Buckhorn Conglomerate Member or the Brushy Basin Member (Fig. 7A). In some locations the calcrete zone consists of gray/purple carbonate nodules up to 40 cm in diameter (Fig. 7A). These nodules are enclosed in a purple-green, sandy mudstone matrix. Large nodules are locally coalesced into laterally continuous beds up to 10 m thick, or are separated by 1–10 cm of enclosing matrix. These nodules contain massive to concentrically laminated, microcrystalline and sparry calcite encompassing smaller ($<$ 3 cm), brecciated or laminated nodules. Small vugs and thin veins of sparry calcite and silica are common. These nodules may contain partially replaced sand grains or streaks of argillaceous material.

Laminar to structureless calcrete zones consist of up to 10 m of white/gray micritic to sparry and pisolitic calcrete. These calcretes consist of structureless sparry and microcrystalline calcite that partially and fully replaces detrital grains. In many cases large chert pebbles can be observed floating in a micritic matrix (Fig. 7B). In addition, the massive calcrete contains small (1–20 mm) nodules of angular and concentrically laminated sparry and microcrystalline calcite. The small indurated nodules also contain partially replaced sand grains of the host sediment. In many locations, structureless and laminar calcrete overlies nodular calcrete horizons.

The nodular and massive calcretes at the base of the upper Cedar Mountain are interpreted as a mature pedogenic carbonate (Stages V or VI of Machette 1985) that formed during development of an unconformity following deposition of the Buckhorn Conglomerate Member. The thick and well indurated nature of the calcrete zone may reflect early diagenesis and recrystallization due to fluctuating groundwater levels and changes in groundwater chemistry (e.g., Arakel 1986; Khalaf 1990; Spötl and Wright 1992). Whether formed by primary pedogenic processes or later groundwater modification, the presence of the basal calcrete indicates an arid to semiarid climate during the time of formation. The widespread distribution and great thickness of the calcrete zone suggests that it formed at a time of little or no deposition in the study area. Modern calcretes with similar characteristics form on landscapes that have been dominantly nonaggradational for $>$ 5 m.y. (Machette 1985). As such, this calcrete zone may represent a regional unconformity that developed following deposition of the Buckhorn Conglomerate.

Above the basal calcrete zone, the upper Cedar Mountain Formation consists of 10–30 m of mudstone, sandstone, and minor limestone (Table 2). Upper Cedar Mountain sediments are the deposits of a poorly drained, fluvial/lacustrine plain. Mudstone in the upper Cedar Mountain Formation

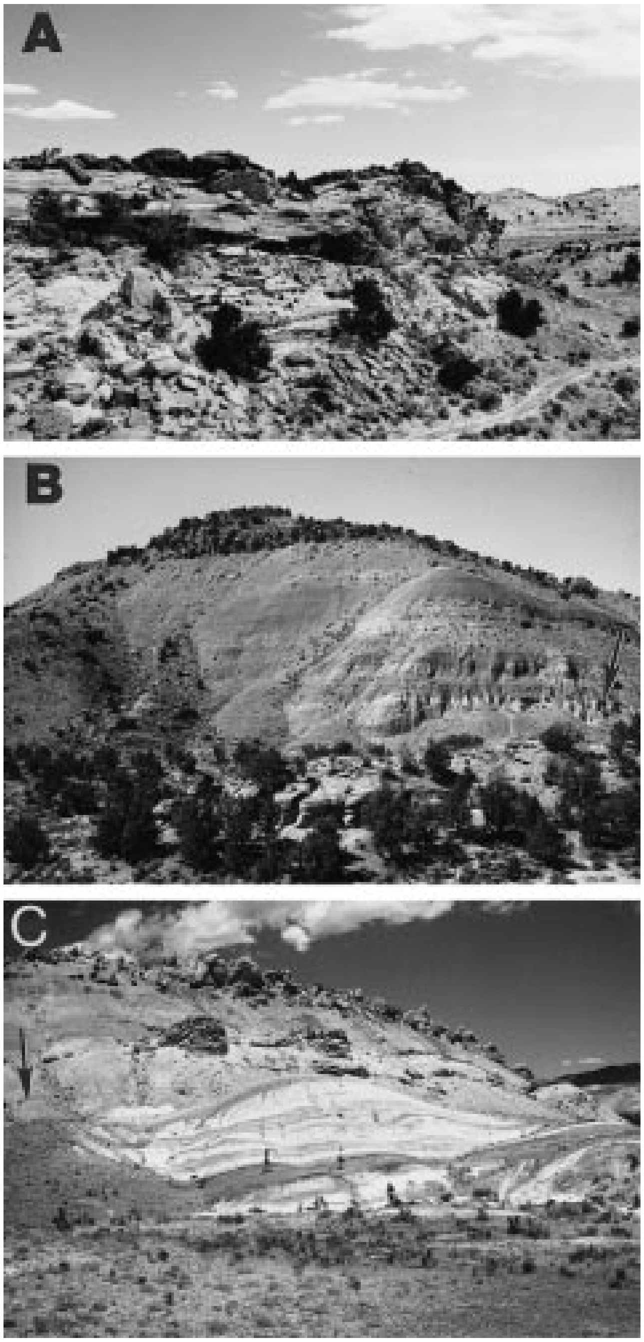

FIG. 4.—Outcrop photographs of the Morrison Formation. **A)** Upper Salt Wash Member braided fluvial channel sandstone at 1FD section. Sandstone is ~ 25 m thick at this location. **B)** Lower and middle part of the Brushy Basin Member, TCW section. Arrow points to boundary between the two units. Middle Brushy Basin fluvial channel crops out near the top of the hill. Hill is capped by the Buckhorn Conglomerate. **C)** Altered, upper part of the Brush Basin Member near 2IP section. Arrow marks the contact between the Morrison and Cedar Mountain Formations. Cedar Mountain fluvial channel sandstones crop out halfway up the slope, and the ridge is capped by Dakota Formation sandstone.

is interpreted as overbank sediment that accumulated on the alluvial plain during floods. The massive nature of the mudstones and the horizons of nodular carbonate indicate pedogenic modification of overbank material. The thin micritic limestone beds within the unit are interpreted as shallow lacustrine deposits. The lenticular sandstone bodies are deposits of laterally stable fluvial channels. Paleocurrent data from these sandstone bodies indicate a northeastward transport direction (Fig. 5D). The lack of lateral accretion surfaces and the laterally discontinuous nature of the channel bodies suggest that the main form of channel migration was by avulsion. The general increase in channel size, decrease in carbonate nodules, and preserved carbonaceous material in mudstones near the top of the formation indicate that climate may have been more humid in the late stages of Cedar Mountain deposition relative to conditions during formation of the basal calcrete.

Summary

The Morrison Formation can be subdivided into three related facies assemblages. The first of these contains the Windy Hill, Tidwell, and lower Salt Wash Members. These units were deposited as shallow marine, tidal, lacustrine, fluvial, and eolian facies following retreat of Redwater Member marine depositional systems. The second assemblage consists of upper Salt Wash Member sandy and gravelly braided fluvial facies, and lower Brushy Basin Member meandering fluvial facies. The upper Salt Wash records increasing amalgamation of fluvial channel facies and progradation of coarse-grained material into the study area from the west. The lower unit of the Brushy Basin Member represents decreasing fluvial gradients and floodplain stabilization that resulted in generation of well developed paleosols. The third Morrison assemblage is composed of the stable, low-sinuosity, fluvial channel facies of the middle and upper units of the Brushy Basin Member. Smectitic mudstone and bentonite beds in the middle Brushy Basin indicate a probable volcanic source for much of the fine-grained sediment. The upper part of this assemblage shows evidence of sediment alteration and early diagenesis related to development of the regional K unconformity of Pipiringos and O'Sullivan (1978).

The overlying Cedar Mountain Formation can be divided into two facies assemblages. The first of these consists of the Buckhorn Conglomerate Member, which was deposited by a northeast-trending gravelly fluvial system that filled a 25 km wide valley incised into the underlying Brushy Basin Member. The upper parts of the Buckhorn Conglomerate Member contains finer-grained sediments associated with the late stages of valley fill. The second facies assemblage consists of upper Cedar Mountain Formation low-sinuosity fluvial and lacustrine facies. This assemblage is separated from the underlying Buckhorn Conglomerate and Brushy Basin Member by a possible unconformity marked by a regionally extensive nodular to massive calcrete horizon.

SEDIMENTARY PETROLOGY

Methods

Sixty-eight standard petrographic thin sections of Morrison and Cedar Mountain sandstone from the study area were point counted using the Gazzi–Dickinson method (Ingersoll et al. 1984). Thin sections were stained for both potassium and plagioclase feldspars, and at least 450 grains per slide were counted. The point-counting parameters are listed in Table 3.

Results

Sandstones in the Morrison and Cedar Mountain formations contain quartz, feldspar, and various lithic grains. Quartz grains range from very fine to very coarse, and are principally well rounded, nonundulose, and monocrystalline (Qm). Feldspar (F) is present as monocrystalline, coarse- to fine-sand grains that are moderately to well rounded. Potassium feldspar (K), including microcline and orthoclase, constitutes the majority of feldspar in most samples, although plagioclase (P) is abundant in some samples. The lithic (Lt) component of Morrison and Cedar Mountain sandstones consists primarily of chert (C) grains with lesser proportions of

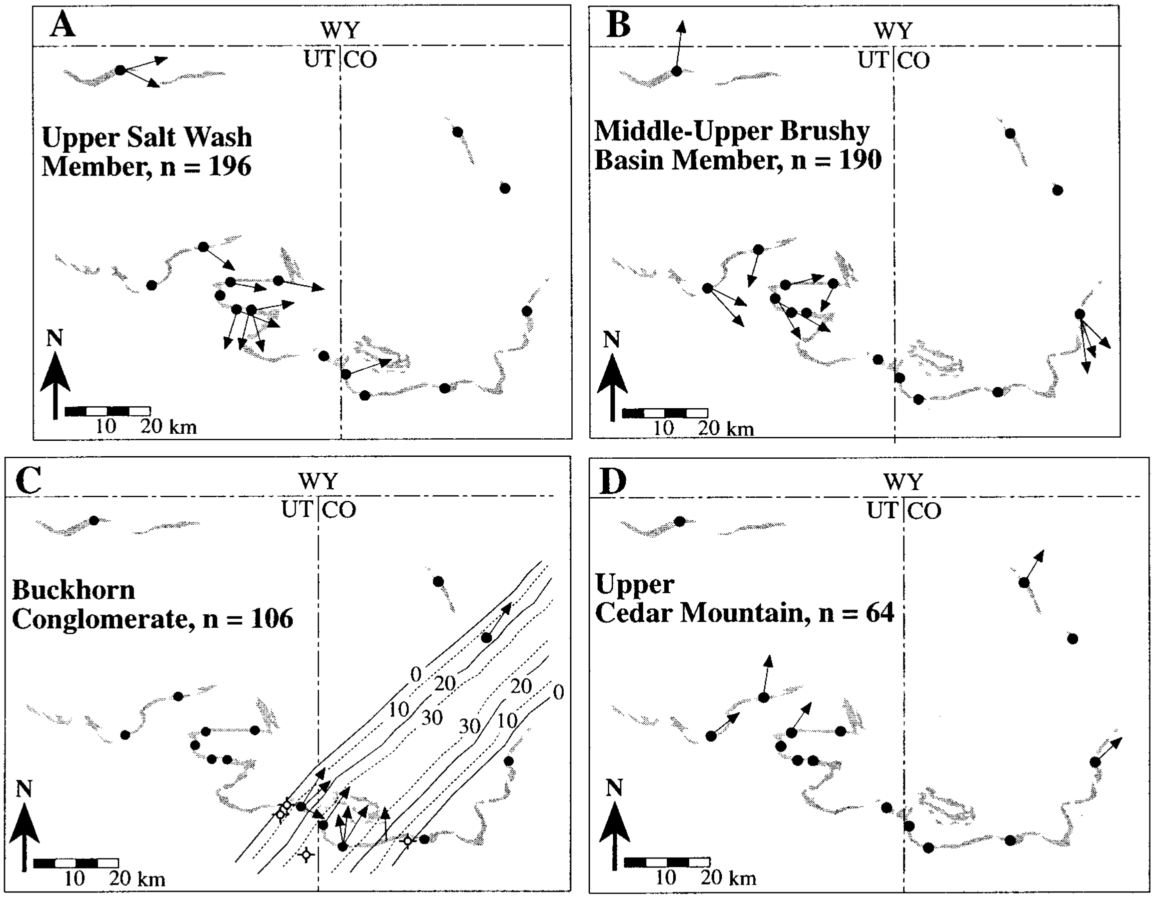

FIG. 5.—**A)** Paleocurrent orientations from the upper Salt Wash Member at measured section locations (dark circles) in the study area. Each arrow represents the average trough axis determined from 10 or more measurements of trough limbs per station according to method I of DeCelles et al. (1983). **B)** Paleocurrent orientations from the upper Brushy Basin Member in the study area. **C)** Paleocurrent and isopach map of the Buckhorn Conglomerate Member in the study area showing northeast-trending distribution of the unit. Open circles represent well locations used in subsurface thickness calculations. Isopach thickness is in meters. **D)** Paleocurrent orientations from the upper Cedar Mountain Formation in the study area.

polycrystalline quartz (Qp) and volcanic lithic (Lv) grains. Volcanic lithic grains consist of altered vitric tuff fragments. In most grains, original textures have been altered to smectitic clays, but some exhibit vitric shards and remnant flow textures. Small feldspar phenocrysts, opaque microlites, euhedral biotite crystals, and aggregates of small quartz crystals are present in some Lv grains. Chert types include pure, spicular, fossiliferous, chalcedonic, and silty varieties. Qp grains are composed of very fine- to coarse-sand grains that contain polygonized, elongate, and sutured crystals.

Recalculated point-count data from the Morrison and Cedar Mountain formations are listed in Table 4. Compositionally, these sandstones can be divided into three petrofacies: a lower Morrison petrofacies, an upper Morrison petrofacies, and a Buckhorn/Cedar Mountain petrofacies. The lower Morrison petrofacies includes sandstones from the Windy Hill, Tidwell, and lower Salt Wash Members; the upper Morrison petrofacies includes sandstones from the upper Salt Wash and Brushy Basin Members (Fig. 8A, B).

The lower Morrison petrofacies has average framework compositions of %QFL = 79, 19, 2; %QmFLt = 70, 19, 11; and %QmFC = 74 , 20, 6. The average ratio of plagioclase to total feldspar is 0.41. Lithic components in lower Morrison sandstones consist of subequal proportions of chert and polycrystalline chert with lesser amounts of lithic volcanics (average %QpLvC = 34, 20, 46).

The upper Morrison petrofacies has average framework compositions of %QFL = 92, 5, 3; %QmFLt = 54, 5, 41; %QmFC = 59, 5, 36. The average ratio of plagioclase to total feldspar is 0.33. Lithic grains from the upper Morrison sandstones are dominated by chert, with the average C/Lt = 0.78. Sandstones from the upper Morrison petrofacies also contain the largest average percentage of lithic volcanic fragments found in the Morrison–Cedar Mountain stratigraphic section, with average %Lv/total framework grains = 3.

The Buckhorn/Cedar Mountain petrofacies has average framework compositions of %QFL = 95, 4, 1; %QmFLt = 69, 4, 27; and %QmFC = 72, 4, 24. The average ratio of plagioclase to total feldspar is 0.34. Although similar, Buckhorn/Cedar Mountain sandstones are distinguished from upper Morrison sandstone by their increased content of quartz and decreased content feldspar, chert, and lithic volcanics.

Provenance Interpretation

Morrison sandstones lie within the ''continental block'' and ''recycled orogen'' provenance fields of Dickinson et al. (1983), whereas Cedar Mountain sandstones lie entirely within the recycled orogen field. The indication of both a continental block and recycled orogen provenance for Morrison sandstones suggests that there may be a possible mixture of source-area rock types. The presence of potassium feldspar in both Morrison and Cedar Mountain sandstones indicates derivation from several pos-

FIG. 6.—**A)** Outcrop of Buckhorn Conglomerate Member at 1MHQ section. **B)** Close-up photograph of Buckhorn Conglomerate at 1MHQ section. Scale is in centimeters (left) and inches (right).

sible sources, including Precambrian basement rocks, Mesozoic plutonic rocks, and reworked Mesozoic–Paleozoic arkosic sedimentary rocks. The high quartz content of these sandstones denotes a contribution of mature sediment from weathered basement rocks or reworked quartzose sandstones. The abundance of chert grains indicates weathering of supracrustal sedimentary rocks, whereas volcanic rock fragments suggest a magmatic-arc-related source.

Source-area locations can be inferred through evaluation of Morrison–Cedar Mountain sediment dispersal pathways. Paleocurrent data from the Morrison indicate sediment transport from a western source area, whereas Buckhorn and Cedar Mountain detritus was transported from the southwest (Fig. 5). In view of the paleocurrent data, a Precambrian basement source for quartz and feldspar in the Morrison and Cedar Mountain formations is unlikely. Possible causes of early uplift in the Cordillera west of the study

TABLE 3.—*Petrographic point-counting parameters.*

Symbol	Definition
Raw Parameters	
Qm	monocrystalline quartz
Qp	polycrystalline quartz
P	plagioclase
K	potassium feldspar
Lv	volcanic rock fragments
Ls	fine-grained sedimentary rock fragments
C	chert, including chalcedony
Recalculated Parameters	
Q	total quartzose grains (Qm + Qp + C)
F	total feldspar (P + K)
L	total unstable lithic grains (Lv + Ls)
Lt	Lv + Ls + C + Qp

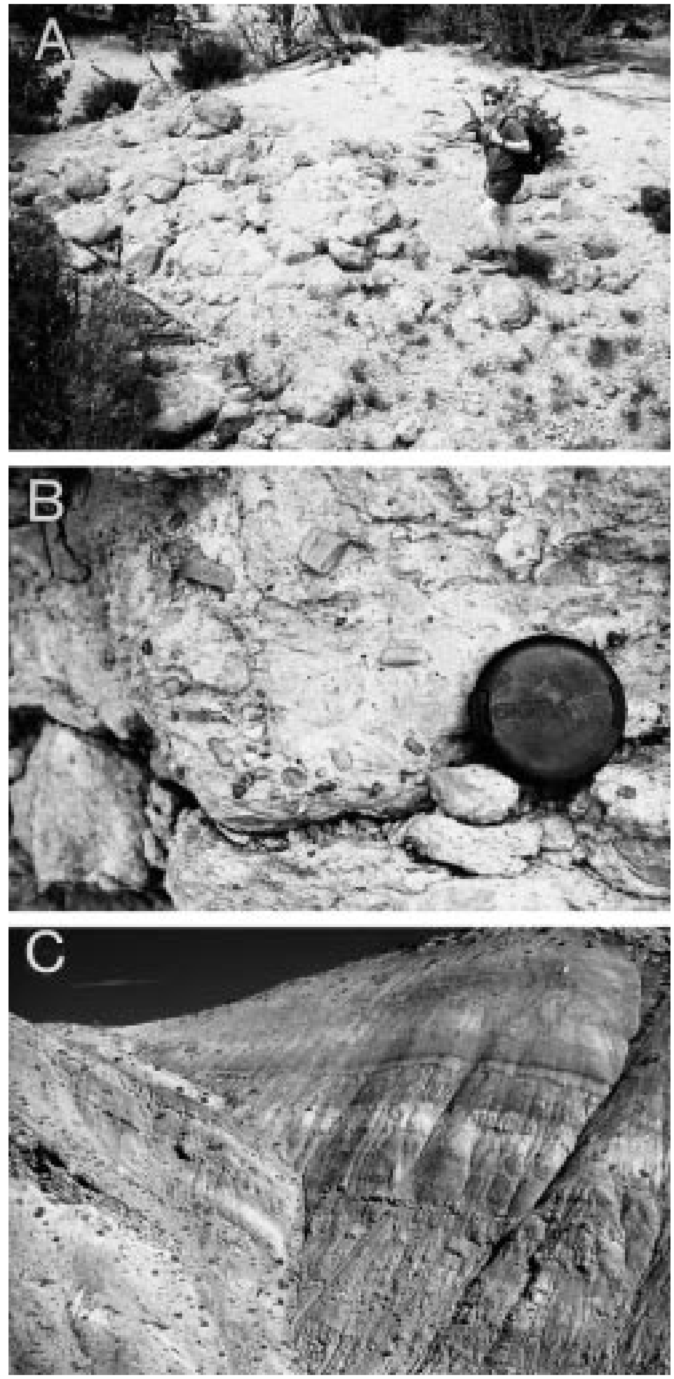

FIG. 7.—**A)** Large calcrete nodules from the base of the upper Cedar Mountain Formation weathering out of a hillslope near 1DP section. **B)** Close-up of massive calcrete at 1DP section showing chert pebbles floating in micritic calcrete matrix. **C)** Fine-grained interval in the Cedar Mountain Formation at 1OD section displaying numerous nodular carbonate horizons in the lower two-thirds of the outcrop. Mudstone in the upper third of the outcrop is carbonaceous and contains no nodular carbonate.

TABLE 4.—*Recalculated point-count data from Morrison and Cedar Mountain formation sandstones.*

		% QFL			% QmFLt			% QmFC				
Sample*	Member†	Q	F	L	Qm	F	Lt	Qm	F	C	% Lv	P/P + K
Lower Morrison Petrofacies												
1RF 0.6	wh	75.90	23.70	0.40	72.90	23.71	3.39	73.20	23.80	3.00	0.40	0.48
1RF 1.3	wh	78.32	21.02	0.66	74.78	21.02	4.20	75.79	21.30	2.91	0.66	0.44
1IP 3.2	w	72.32	27.46	0.22	60.71	27.46	11.83	66.50	30.08	3.42	0.22	0.29
1RF 10.1	t	83.19	13.90	2.91	74.67	13.90	11.43	81.22	15.12	3.66	2.91	0.47
1RF 15.5	t	75.71	20.13	4.16	69.80	20.13	10.07	74.88	21.60	3.52	4.61	0.33
1IP 6.8	t	72.12	27.65	0.23	66.60	27.65	5.75	69.52	28.86	1.62	0.22	0.38
1IP 12.5	t	76.35	21.85	1.80	71.17	21.85	6.98	74.35	22.82	2.83	1.80	0.33
1IP 13.2	sl	88.33	7.49	4.18	70.04	7.49	22.47	78.91	8.44	12.65	4.19	0.59
1IP 20.5	sl	89.86	5.86	4.28	50.22	5.86	43.92	57.62	6.72	35.66	4.28	0.46
1IP 32.4	sl	70.60	26.73	2.67	65.03	26.73	8.24	68.87	28.30	2.83	2.67	0.37
1IP 36.2	sl	69.62	27.66	2.72	66.90	27.66	5.44	69.58	28.77	1.65	2.72	0.40
1IP 37.0	sl	79.78	18.44	1.78	74.89	18.44	6.67	79.29	19.53	1.18	1.78	0.55
1IP 38.9	sl	69.33	30.67	0.00	66.31	30.67	3.02	67.92	31.42	0.66	0.00	0.44
1IP 49.4	sl	78.93	19.96	1.11	76.71	19.96	3.33	77.93	20.27	1.80	1.11	0.48
TCW 38.0	sl	90.22	8.00	1.78	80.00	8.00	12.00	84.71	8.47	6.82	1.78	0.22
1DP 30.0	sl	87.12	10.44	2.44	72.45	10.44	17.11	77.25	11.14	11.61	2.44	0.26
Upper Morrison Petrofacies												
1FD 70.0	su	94.22	0.89	4.89	81.11	0.89	18.00	88.59	0.97	10.44	4.89	0.25
1RF 41.0	su	89.58	5.76	4.66	69.63	5.76	24.61	77.92	6.45	15.63	4.66	0.27
1RF 41.1	su	93.67	2.53	3.80	39.66	2.53	57.81	45.41	2.90	51.69	3.80	0.25
1RF 59.0	su	97.43	0.21	2.36	25.70	0.21	74.09	28.17	0.23	71.60	2.36	0.00
1RF 81.9	su	92.43	3.56	4.01	22.94	3.56	73.50	28.37	4.41	67.22	4.01	0.56
1RF 84.5	su	94.28	0.88	4.84	27.69	0.88	71.43	31.97	1.02	67.01	4.84	0.25
1IP 52.7	su	90.00	5.78	4.22	56.22	5.78	38.00	61.25	6.30	32.45	4.22	0.50
1IP 52.8	su	90.66	8.43	0.91	55.81	8.43	35.76	69.02	10.42	20.56	0.91	0.41
1IP 53.8	su	84.10	8.06	7.84	55.99	8.06	35.95	69.46	10.00	20.54	7.84	0.27
1IP 63.0	su	94.26	3.31	2.43	55.41	3.31	41.28	66.75	3.99	29.26	2.43	0.40
1IP 70.5	su	96.73	2.10	1.17	40.89	2.10	57.01	43.86	2.26	53.88	1.17	0.22
1RF 102.5	bl	77.54	20.08	2.38	73.43	20.09	6.48	76.75	20.99	2.26	2.38	0.41
1RF 110.0	bl	96.84	3.16	0.00	20.99	3.16	75.85	22.35	3.37	74.28	0.00	0.71
TCW 97.5	bl	85.33	12.89	1.78	74.67	12.89	12.44	81.16	14.01	4.83	1.78	0.26
1RF 136.8	bm	82.70	13.97	3.33	78.49	13.97	7.54	82.51	14.69	2.80	3.33	0.49
1RF 144.7	bm	78.20	17.75	4.05	70.12	17.75	12.13	76.10	19.27	4.63	4.04	0.42
1RF 160.1	bm	82.73	7.95	9.32	63.64	7.95	28.41	74.07	9.26	16.67	9.32	0.57
2IP 156.5	bm	88.22	6.00	5.78	72.67	6.00	21.33	79.95	6.60	13.45	0.00	0.30
1TD 179.0	bm	90.45	6.44	3.11	70.00	6.44	23.56	77.78	7.16	15.06	3.11	0.14
1TD 179.9	bm	93.55	1.56	4.89	54.66	1.56	43.78	59.56	1.70	38.74	4.89	0.00
TCW 155.0	bm	88.89	1.78	9.33	39.55	1.78	58.67	45.41	2.04	52.55	9.33	0.25
RWD 146.0	bm	93.56	2.00	4.44	55.33	2.00	42.67	58.59	2.12	39.29	4.44	0.33
1FD 194.0	bu	94.23	3.33	2.44	74.00	3.33	22.67	77.99	3.51	18.50	2.44	0.07
1FD 196.0	bu	95.55	3.56	0.89	61.33	3.56	35.11	63.74	3.70	32.56	0.89	0.00
1SC 22.0	bu	99.11	0.22	0.67	22.72	0.22	77.06	25.50	0.25	74.25	0.67	1.00
1SR 1.6	bu	97.35	2.21	0.44	73.07	2.21	24.72	75.57	2.28	22.15	0.44	0.70
1RF 190.0	bu	82.89	13.11	4.00	66.67	13.11	20.22	71.26	14.01	14.73	4.00	0.47
1SMA 1.6	bu	96.66	1.11	2.23	23.39	1.11	75.50	25.80	1.23	72.97	2.23	0.40
1SMA 14.5	bu	98.66	0.67	0.67	52.44	0.67	46.89	56.59	0.72	42.69	0.67	0.33
1SMA 22.6	bu	96.44	3.56	0.00	78.88	3.56	17.56	81.24	3.66	15.10	0.00	0.44
1SMA 30.4	bu	99.78	0.00	0.22	37.11	0.00	62.89	38.75	0.00	61.25	5.78	0.00
1SMA 32.5	bu	99.33	0.00	0.67	47.78	0.00	52.22	52.18	0.00	47.82	0.22	0.00
2IP 196.0	bu	99.56	0.22	0.22	15.11	0.22	84.67	16.31	0.24	83.45	5.78	0.00
2IP 202.5	bu	96.89	2.67	0.44	83.55	2.67	13.78	86.64	2.76	10.60	0.22	0.33
1IP 196.6	bu	95.99	2.23	1.78	37.86	2.23	59.91	42.07	2.48	55.45	1.78	0.60
Cedar Mountain Petrofacies												
TCW 186.0	bc	96.44	2.67	0.89	67.33	2.67	30.00	72.49	2.87	24.64	0.89	0.17
IBC 152.0	bc	98.89	1.11	0.00	85.78	1.11	13.11	86.93	1.13	11.94	0.00	1.00
MHQ 136.2	bc	90.67	5.33	4.00	54.45	5.33	40.22	60.19	5.90	33.91	4.00	0.83
MHQ 150.0	bc	99.34	0.22	0.44	64.89	0.22	34.89	68.55	0.23	31.22	0.44	0.00
MHQ 154.0	bc	99.34	0.22	0.44	31.78	0.22	68.00	34.46	0.24	65.30	0.44	0.00
MHQ 164.5	bc	96.65	2.90	0.45	80.81	2.90	16.29	84.58	3.04	12.38	0.45	0.23
1SC 58.5	uc	97.68	1.16	1.16	36.43	1.16	62.41	40.26	1.28	58.46	1.16	0.00
1SR 58.4	uc	90.61	8.95	0.44	86.90	8.95	4.15	88.84	9.15	2.01	0.44	0.66
1RF 234.7	uc	86.27	11.33	2.40	73.64	11.33	15.03	77.52	11.93	10.55	2.40	0.33
1SMA 43.9	uc	93.56	6.44	0.00	61.78	6.44	31.78	65.72	6.86	27.42	0.67	0.38
2IP 238.5	uc	90.00	9.11	0.89	75.78	9.11	15.11	78.94	9.49	11.57	0.44	0.22
2IP 242.0	uc	96.67	2.44	0.89	70.89	2.44	26.67	73.33	2.53	24.14	0.89	0.18
1BC 183.9	uc	94.22	5.56	0.22	82.66	5.56	11.78	85.13	5.72	9.15	0.22	0.44
MHQ 173.5	uc	96.22	3.78	0.00	85.55	3.78	10.67	87.70	3.87	8.43	0.00	0.12
MHQ 187.0	uc	96.89	2.89	0.22	49.11	2.89	48.00	50.58	2.97	46.45	0.22	0.31
1IC 176.0	uc	99.33	0.67	0.00	75.55	0.67	23.78	81.73	0.72	17.55	0.00	0.67
1DP 187.0	uc	98.45	1.33	0.22	83.11	1.33	15.56	90.12	1.45	8.43	0.22	0.17

* Sample labels indicate measured section locations (see Figure 1) and stratigraphic position above the base of the section.
† Member abbreviations are as follows: w = Windy Hill Mbr.; sl = lower Salt Wash Mbr.; su = upper Salt Wash Mbr.; bl = lower Brushy Basin Mbr.; bm = middle Brushy Basin Mbr.; bu = upper Brushy Basin Mbr.; bc = Buckhorn Conglomerate; uc = upper Cedar Mtn.

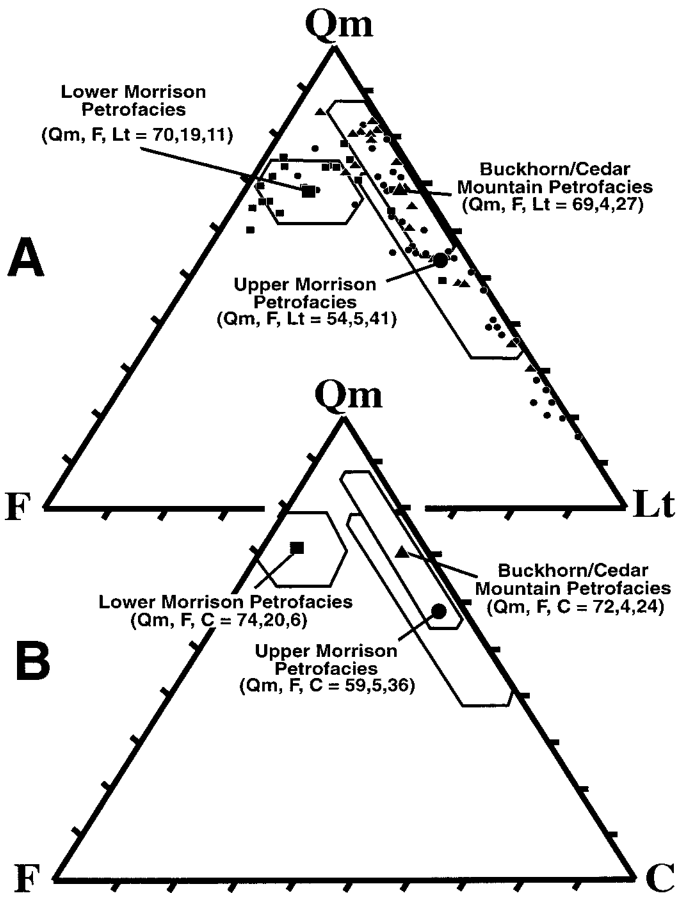

FIG. 8.—Ternary diagrams showing framework compositions of Morrison and Cedar Mountain sandstones in the study area. **A)** QmFLt compositions of lower Morrison (squares), upper Morrison (circles), and Buckhorn/Cedar Mountain (triangles) petrofacies. **B)** Average QmFC plot for Morrison and Cedar Mountain Formation Sandstones showing the dominance of chert in the lithic grain proportions. Polygonal outlines represent the area within one standard deviation of the mean. See Table 3 for definitions of parameters.

area could have involved thrusting, thermal upwarping, or subduction-related generation of topography (Royse et al. 1975; Wiltschko and Dorr 1983; Heller and Paola 1989; Yonkee 1992; Coogan 1992; Lawton 1994). All of these possible causes would have involved erosion of primarily supracrustal rocks. In addition, a Mesozoic plutonic source is also unlikely. Middle and Late Jurassic plutonic rocks that are found today in western Utah and eastern Nevada were probably not broadly unroofed during Morrison and Cedar Mountain deposition (e.g., DeCelles and Burden 1992; Hudec 1992). However, volcanic rocks related to these intrusive bodies may have supplied the volcanic lithic grains that are present in some Morrison and Cedar Mountain sandstones (DeCelles and Burden 1992).

Morrison and Cedar Mountain strata were most likely derived from lower Mesozoic, Paleozoic, and Proterozoic sedimentary rocks to the west and southwest of the study area. Likely sources of the abundant feldspar in lower Morrison sandstones include arkosic sedimentary rocks of the Pennsylvanian–Permian formations in northern Utah and southern Idaho (Allmendinger 1983), the Triassic Ankareh Formation, and Jurassic Nugget and Pruess formations found today in the Utah–Idaho–Wyoming thrust belt (Sippel 1982; DeCelles et al. 1992). The high quartz content of both Morrison and Cedar Mountain sandstones also could have been derived from these arkosic sedimentary rocks, as well as the Pennsylvanian Weber Formation and Oquirrh Group, and Proterozoic–Devonian quartzites in northern and central Utah (Armstrong and Cressman 1963; Hintze 1988). Sources for the abundant chert grains in Morrison and Cedar Mountain sandstones can be found in Paleozoic chert-bearing sedimentary rocks of the Sevier thrust belt and the Cordilleran hinterland in Utah, Nevada, and Idaho (Peterson 1987; Yingling 1987; DeCelles and Burden 1992). Chert-bearing rocks of similar age also are abundant in the hinterland southwest of the study area, the inferred source area of the Buckhorn Conglomerate (Stokes 1944; Yingling and Heller 1992).

The unroofing sequence that would have resulted from erosion of these Proterozoic, Paleozoic, and Mesozoic source rocks generally fits vertical compositional trends found in Morrison and Cedar Mountain sandstones (Fig. 9). Initial erosion of Mesozoic and upper Paleozoic arkosic sediments from source areas west of the study area would account for the high percentage of well-rounded feldspar grains in the lower Morrison petrofacies. Continued erosion and increasing dissection of underlying Carboniferous–Permian chert-bearing rocks would account for the increasing abundance of chert in upper Morrison sandstones.

Although paleocurrent data indicate a shift in sediment dispersal pathways following Morrison deposition, the abundance of upper Paleozoic chert in Buckhorn sandstones and conglomerates suggests a similar unroofing history in source areas to the southwest. The decrease in chert and increase in quartz in upper Cedar Mountain sandstones may have resulted from continued erosion and decreased availability of Upper Paleozoic chert-bearing sediments and the initial exposure of Proterozoic–Devonian quartzites in the source area. This hypothesis is supported by the presence of Proterozoic–lower Paleozoic quartzite clasts in Lower Cretaceous conglomerates in central Utah, to the west of the study area (DeCelles et al. 1995).

An evaluation of the provenance data gives an indication of the timing of initiation of thrusting in the central Cordillera. Earlier workers have suggested that the source for Late Jurassic and Early Cretaceous sediments in the western interior was associated with emplacement of the Paris–Willard thrust sheet in northern Utah and southeastern Idaho (Armstrong and Cressman 1963; Jordan 1981; Wiltschko and Dorr 1983). This interpretation was based primarily on a correlation of the conglomerate at Red Mountain, Idaho with the lower part of the Lower Cretaceous Gannett Group in the Idaho–Wyoming thrust belt (Mansfield 1927; Armstrong and Cressman 1963). A detailed analysis by DeCelles et al. (1993) has shown that the conglomerate at Red Mountain is actually a local facies within the Aptian Bechler Formation, and was produced as a result of initial displacement on the Mead thrust and coeval uplift of the inactive Paris thrust sheet. The age of the Bechler suggests that most of the $\sim$ 60 km displacement on the Paris thrust (Coogan 1992) occurred prior to Aptian time. In addition, $^{40}Ar/^{39}Ar$ ages for sericite in syndeformational veins in the Willard thrust sheet in northern Utah indicate that motion on the Willard thrust occurred between 140–110 Ma (Yonkee 1990). Although this age post-dates deposition of most of the Morrison Formation in the study area, the ages determined may be related to cooling during the later stages of emplacement of the Willard sheet or during initial Meade thrusting (W.A. Yonkee, personal communication 1995). This suggests that uplift and erosion of the Mesozoic and Paleozoic rocks in the hanging wall of the Willard sheet may have supplied Morrison detritus during the Late Jurassic. In addition, two older thrust terranes in western Utah were emplaced prior to Willard thrusting (Camilleri et al. 1997). These thrust sheets also contained Mesozoic and upper Paleozoic rocks that could have contributed most of the grain types in Morrison Formation sandstones and conglomerates (DeCelles and Burden 1992; Camilleri et al. 1997).

On the basis of composition and direction of sediment transport, the Buckhorn Conglomerate and upper Cedar Mountain Formation were most likely derived from Proterozoic–Permian source rocks located southwest of the study area. Likely source terranes include the Canyon Range and Pavant thrust sheets in central Utah, the San Francisco and Wah Wah Mountains

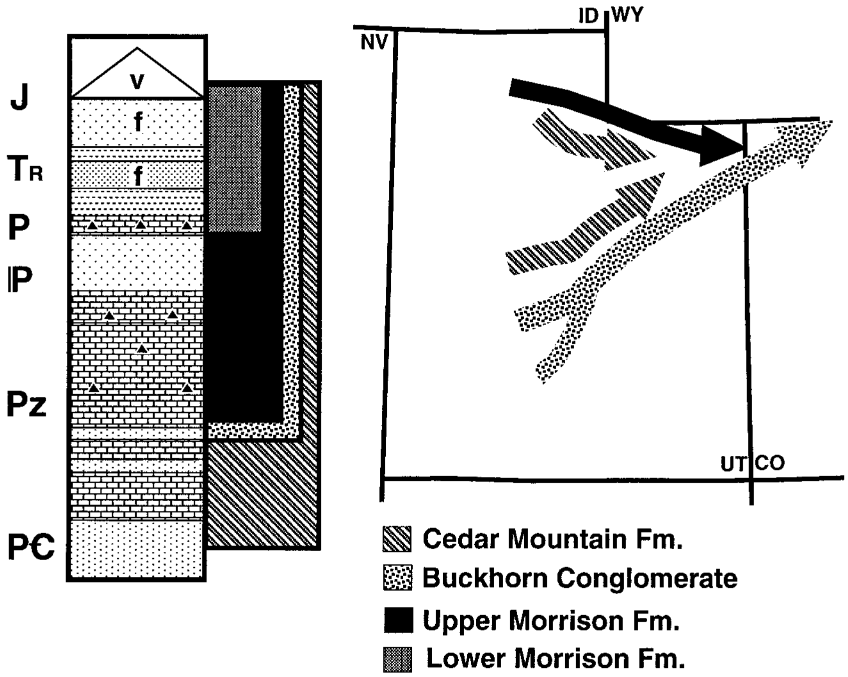

FIG. 9.—Generalized provenance map for the Morrison and Cedar Mountain formations in the study area. Arrows represent direction of sediment transport for the upper Morrison and Buckhorn/Cedar Mountain Formation petrofacies determined by paleocurrent orientations. The column to the left of the map is a schematic representation of the stratigraphic section in the eastern Cordillera, with the age of possible source lithologies for the Morrison and Cedar Mountain petrofacies bracketed by boxes representing each unit. Triangles indicate chert-bearing lithologies; f represents feldspar-bearing rocks; v denotes volcanic sources for both coarse and fine-grained sediment in the Morrison and Cedar Mountain Formations. Note the progressive unroofing of the source area from lower Morrison through Cedar Mountain deposition.

thrust sheets in southwestern Utah, and the Sevier belt of southeastern Nevada (Yingling and Heller 1992; Currie 1994, 1995).

Although the Paleozoic–Proterozoic sedimentary section in the thrust belt could have supplied the majority of grains and clast types found in Buckhorn and Cedar Mountain, Yingling and Heller (1992) indicated that the lack of a westward-thickening correlative to the Buckhorn Conglomerate indicates that thrusting in the Sevier Belt did not begin until deposition of the Cedar Mountain Formation. DeCelles et al. (1995) suggested that thrusting in the central Utah segment of the Sevier belt was initiated with displacement on the Canyon Range thrust during late Neocomian time. This is based on the interpreted age of the Cedar Mountain Formation in the western Wasatch–Gunnison Plateau region. However, conglomerates near the base of the Cedar Mountain Formation along the west flank of the Wasatch Plateau contains Ordovician–Devonian quartzite clasts (DeCelles et al. 1995). This suggests that the source area had been uplifted and unroofed deeply enough to expose the lower Paleozoic section by late Neocomian time. Structural reconstruction of the Canyon Range thrust indicates that a minimum of $\sim$ 40 km of displacement was necessary by late Neocomian time to bring lower Paleozoic rocks in the hanging wall to the surface to be eroded and incorporated as clasts in Cedar Mountain conglomerates (Currie 1997b). This amount of displacement suggests that thrusting in the central Sevier belt began earlier than late Neocomian time, and may have been active during deposition of the Buckhorn Conglomerate and the Morrison Formation. In addition, the fact that the upper Morrison and Buckhorn–Cedar Mountain petrofacies are nearly identical (Fig. 8) indicates that source areas and perhaps uplift mechanisms were similar. This implies that thrusting in the Sevier belt may have been active during Late Jurassic uplift of Morrison Formation source areas.

REGIONAL CORRELATIONS

Figure 9 shows a generalized correlation between the western Wasatch Plateau and San Rafael Swell in central Utah and the study area. This correlation incorporates the author's unpublished stratigraphic data from the San Rafael Swell and Wasatch Plateau regions of central Utah.

Evaluation of measured sections and comparison of paleocurrent data from the Morrison and Cedar Mountain of central Utah indicate depositional settings similar to those in northeastern Utah and northwestern Colorado (Fig. 10). Chronostratigraphic data from the Morrison Formation between the Uinta Mountains region and central Utah indicate similar ages for the Tidwell and Brushy Basin members (Table 1). The only stratigraphic difference between the two areas is the absence of the Windy Hill Member on the San Rafael Swell (Peterson 1994). The base of the Morrison Formation in east-central Utah is defined by a zone of calcic paleosols and gypsum that is overlain by the Tidwell Member (Fig. 11) (Peterson 1988; Demko et al. 1996). Another difference is that paleocurrent indicators in the Salt Wash and Brushy Basin members in the San Rafael Swell region indicate a southwestern sediment source. Conglomerate clast composition and paleodispersal orientations for the Buckhorn Conglomerate and upper Cedar Mountain Formation in central Utah are similar to those found in the study area (e.g., Yingling 1987).

Correlation of the Morrison and Cedar Mountain formations west of the San Rafael Swell poses several problems. In the western Wasatch Plateau and the Gunnison Plateau region, the Lower Cretaceous section consists of the Cedar Mountain and San Pitch Formations (Sprinkel et al. 1998). In this area, the San Pitch is differentiated from the Cedar Mountain Formation on the basis of lithologic differences. The Cedar Mountain in the Wasatch/Gunnison Plateau region consists of variegated mudstone with abundant calcareous nodules similar to the Cedar Mountain Formation in the San Rafael Swell region (Sprinkel et al. 1998). The San Pitch Formation is coarser grained than the underlying Cedar Mountain and contains interbedded conglomerate, sandstone, and mudstone (Sprinkel et al. 1998).

In the Wasatch/Gunnison Plateau region, the Cedar Mountain Formation rests unconformably on the Oxfordian Twist Gulch Formation (Willis 1986; Schwans 1988). The Morrison Formation and Buckhorn Conglomerate are absent from this area (Stokes 1972; Weiss and Roche 1988; Yingling and Heller 1992). Along the west flank of the Wasatch Plateau at Salina Canyon, the Cedar Mountain and San Pitch Formations consist of 280 m of conglomerate, sandstone, and mudstone (Fig. 10). Weiss and Roche (1988), Yingling and Heller (1992), and Sprinkel et al. (1998) correlated the Cedar Mountain/San Pitch formations with the Cedar Mountain of the San Rafael Swell on the basis of lithologic similarity and fossil age assemblage.

The absence of the Morrison Formation and Buckhorn Conglomerate

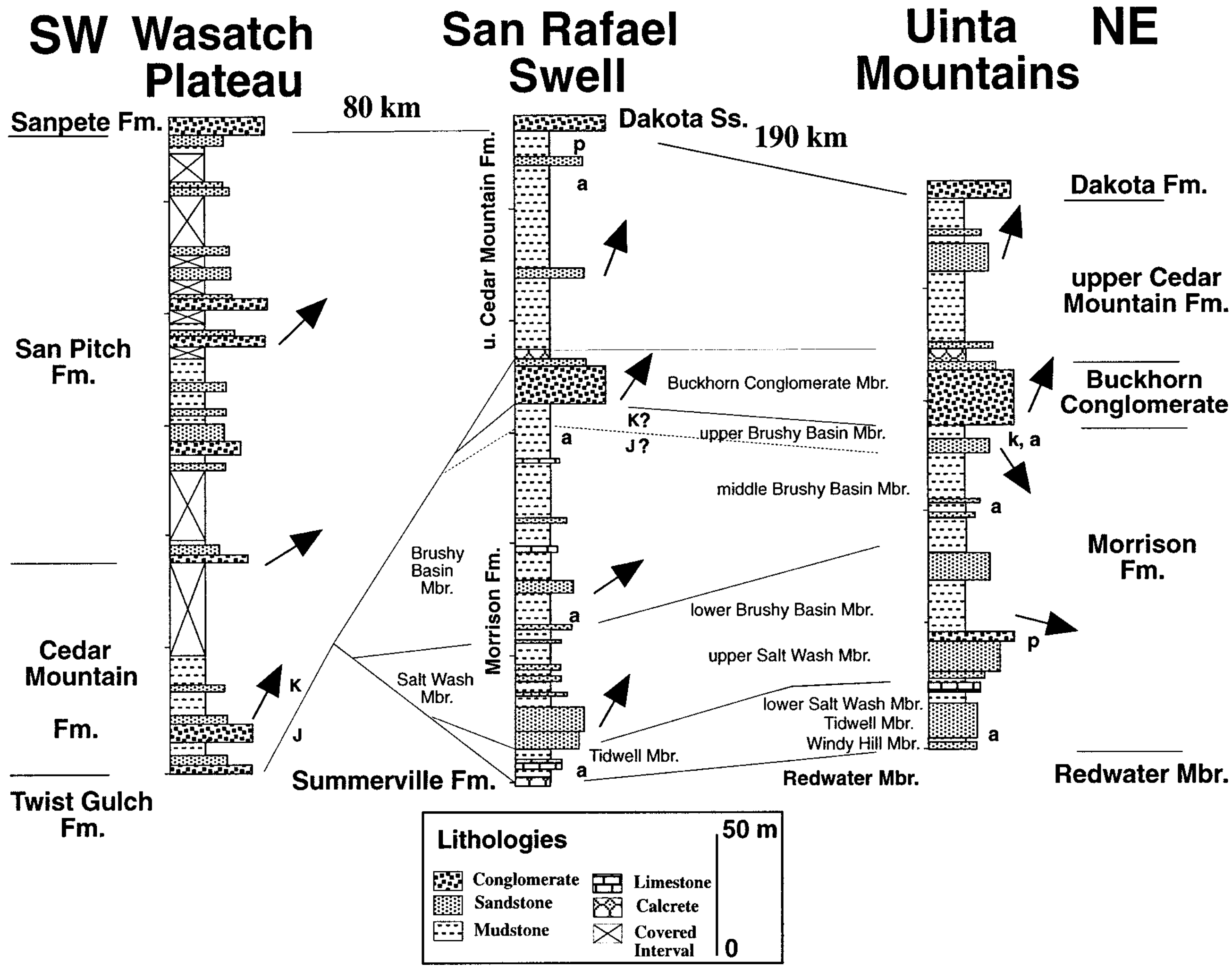

FIG. 10.—Generalized regional correlation diagram of Upper Jurassic–Lower Cretaceous nonmarine rocks between the study area and the Wasatch Plateau in Central Utah. Correlation between members and formations incorporates lithostratigraphic and chronostratigraphic data referred to in the text. Symbols used on the diagram are: arrows, representative paleocurrent orientations from studied areas; a, stratigraphic levels of bentonites dated by $^{40}Ar/^{39}Ar$; p, stratigraphic levels of age-diagnostic palynomorph-bearing mudstones; k, stratigraphic level of K/Ar dated bentonite horizon; K/J indicates the approximate level of the Jurassic–Cretaceous boundary in the upper Morrison Formation. Ages of formations and members are listed in Figure 2 and Table 1.

west of the Wasatch Plateau can be attributed to both nondeposition and postdepositional erosion (Fig. 11). Along the southwestern flank of the San Rafael Swell, both units rest directly on the Middle Jurassic Summerville Formation (Peterson 1988; Currie 1994), an eastern correlative to the Twist Gulch Formation. The Tidwell and Salt Wash members pinch out to the east of this area, indicating that during the Late Jurassic, the Wasatch Plateau was at the western margin of the basin that was eventually filled by Morrison sediments. However, a fluvial lag at the base of the Cedar Mountain Formation at Salina Canyon contains cobble-size clasts of conglomerate and authigenic silica that are similar to beds in the Brushy Basin Member on the San Rafael Swell, suggesting that the upper parts of the Morrison were deposited at this location but were later removed by erosion prior to Cedar Mountain deposition. The cause of this erosion can only be inferred, but it may be related to uplift associated with thermal doming in the hinterland prior to Sevier thrusting (Yingling 1987; Heller and Paola 1989), isostatic uplift of the Cordilleran foreland during a period of Early Cretaceous tectonic quiescence (Heller and Paola 1989; Bjerrum and Dorsey 1995), subduction-related dynamic plateau uplift (Lawton 1994), or migration of a flexural forebulge associated with eastward propagation of the thrust belt during the Early Cretaceous (Currie 1994) (see Discussion). Following this uplift, renewed basin subsidence allowed deposition of the Cedar Mountain Formation directly on the Twist Gulch Formation.

DISCUSSION

The relationship between Late Jurassic–Early Cretaceous deposition and development of the early Cordilleran foreland basin is controversial. Because the Morrison Formation and Buckhorn Conglomerate pinch out in central Utah, deposition of these units in a retroarc foreland-basin setting has been challenged (Heller and Paola 1989; Yingling and Heller 1992; Lawton 1994; Bjerrum and Dorsey 1995). Four possible basin types have been proposed to account for Morrison and Buckhorn deposition. These include a nonmarine basin adjacent to a Late Jurassic–Early Cretaceous thermally generated uplift or isostatically rebounding highland in the Sevier hinterland (Fig. 11A, B; Yingling 1987; Heller and Paola 1989; Bjerrum and Dorsey 1995); a basin formed in response to subduction-generated dynamic subsidence (Fig. 12A; Lawton 1994); a distal foreland setting associated with overfilling of a Middle Jurassic foreland basin (Fig. 12C;

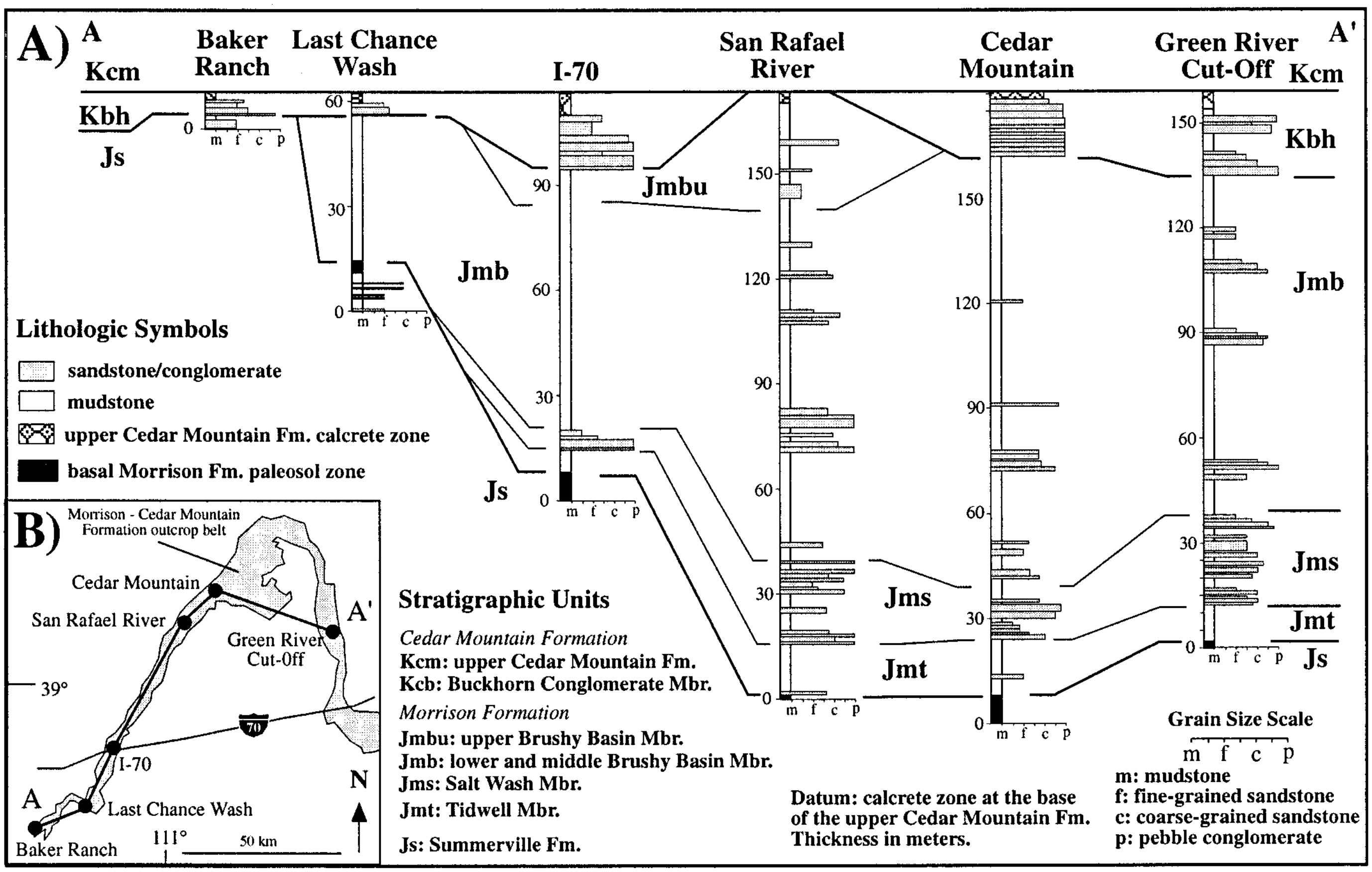

FIG. 11.—**A)** Stratigraphic cross section of the Morrison Formation and Buckhorn Conglomerate on the San Rafael Swell in east-central Utah. The western pinchout of the interval is interpreted as being produced by younger units onlapping a topographic high along the west flank of the San Rafael Swell. **B)** Line of stratigraphic section depicted in (A). See Appendix 1 for section locations.

DeCelles and Burden 1992); and a back-bulge setting associated with cratonward migration of a foreland-basin system during the Late Jurassic and Early Cretaceous (Fig. 12D; Currie 1994).

In considering which basin model is applicable to the Late Jurassic and earliest Cretaceous of the western interior, both the onlapping and erosional western pinchout of the Morrison Formation must be explained (Fig. 11). If the thermal or isostatic-rebound uplift mechanisms apply, two phases of Late Jurassic–Early Cretaceous uplift are required in regions west of the Wasatch Plateau. An initial phase of uplift prior to Morrison deposition is necessary to account for the westward onlap of the formation, and a second, post-Morrison phase is required to produce the erosional truncation of the formation. Although this complex uplift history is possible, there is no evidence of a Late Jurassic–Early Cretaceous deformational hiatus that would be necessary to produce regional isostatic uplift of the Sevier hinterland (DeCelles and Currie 1996). In addition, there is no mechanism to accommodate sediment in the areas east of the uplift.

The generation of dynamic topography associated with a shallowing angle of oceanic plate subduction (cf. Mitrovica et al. 1989; Gurnis 1992) is also an unlikely cause for the stratigraphic relationships observed in the Morrison Formation. Lawton (1994) called on the model proposed by Gurnis (1992) to account for the depositional pinch-out of the Morrison Formation, the asymmetric subsidence observed in the Middle Jurassic rocks of central Utah, and uplift of Paleozoic–Mesozoic source rocks in the Sevier hinterland. In Lawton's application of the model, a decrease in the angle of oceanic plate subduction along the western margin of North America during the Middle Jurassic resulted in uplift of a broad plateau in the present-day Sevier hinterland. This uplift was accompanied by dynamic subsidence of the foreland in central Utah due to viscous flow within the mantle wedge. Continued shallowing of the subducting plate during the Late Jurassic uplifted the foreland and produced depositional offlap of the Morrison Formation in central Utah.

Although the model proposed by Gurnis (1992) predicts dynamic subsidence of the foreland during a decrease in the angle of subduction, it does not generate synchronous uplift of a broad plateau that would serve as a sediment source area. Plateau uplift in the model occurs during the final stages of plate shallowing, when dynamic subsidence in the foreland ceases. In addition, the topography generated by this uplift is a result of inverting basin sediments initially deposited in the dynamically subsiding foreland. For this reason, it is unlikely that the uplift that exposed Paleozoic rocks in Cordilleran sediment source areas was caused by subducted-slab effects. Dynamic subsidence may have produced the accommodation that allowed Middle–Late Jurassic deposition across the region, but it cannot account for the uplift of the Cordilleran source areas.

The overfilled-foreland model of DeCelles and Burden (1992) also cannot completely explain the stratigraphic relationships observed in the Morrison Formation. In this model, both the Morrison and Buckhorn should at some point thicken to the west. Although postdepositional erosion may account for thinning of the units, there is no mechanism in this model to account for the western stratigraphic onlap observed in the Morrison.

Of the models above, the westward pinch-out of the Morrison Formation, as well as the stratigraphic relationships observed in the entire Upper Ju-

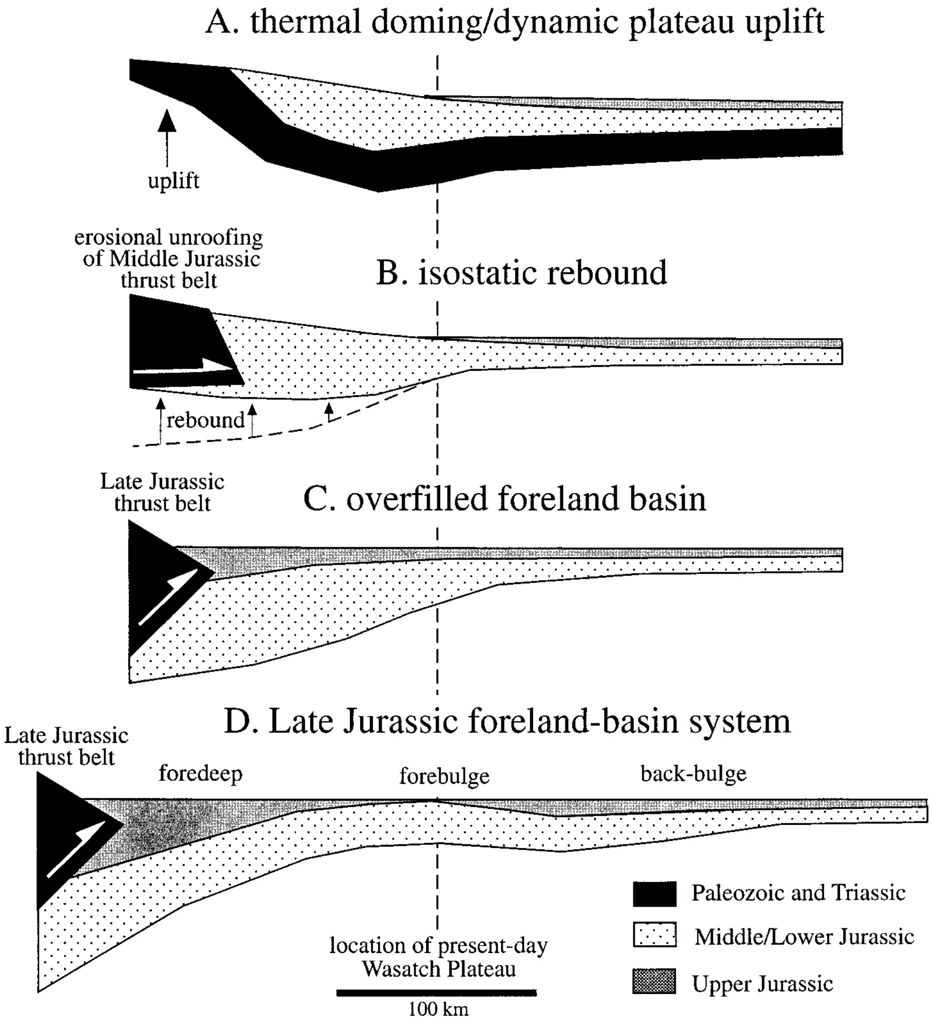

FIG. 12.—Schematic west–east cross sections of Utah during Morrison Formation deposition, showing proposed tectonic settings of the source area and basin. **A)** Morrison deposition occurred in a basin graded to a thermal or dynamic plateau uplift in western Utah and eastern Nevada (modified from Heller and Paola 1989). **B)** Morrison deposition occurred in a basin graded to an isostatically uplifted highland following Middle Jurassic thrusting and foreland-basin development (modified from Heller and Paola 1989). **C)** Morrison deposition in central and eastern Utah occurred in the overfilled part of the Middle–Late Jurassic foreland basin (modified from DeCelles and Burden 1992). **D)** Morrison deposition occurred in the forebulge and back-bulge depozones of the Late Jurassic foreland-basin system.

rassic and Lower Cretaceous sequence in eastern Utah and western Colorado, can be best explained by cratonward migration of a flexural forebulge during the Late Jurassic and Early Cretaceous (e.g., DeCelles and Giles 1996). In this model, aspects of dynamic subsidence (Lawton 1994) and foreland overfilling (DeCelles and Burden 1992) are combined with foreland-basin system flexural components associated with early thrusting in the Cordillera.

During Middle Jurassic time, accommodation in central Utah was produced primarily by subduction-generated dynamic subsidence (Lawton 1994; Currie 1997b). During the Late Jurassic, initiation of thrusting in western Utah resulted in uplift and erosion of Paleozoic–Mesozoic rocks. The crustal loading that accompanied this thrusting led to development of a flexurally subsiding foredeep in western Utah and uplifted forebulge in central Utah (Fig. 13A). Between the forebulge and the undeformed craton a secondary back-bulge basin also developed. As the developing foreland became overfilled, sediment from the Cordillera was transported across the crest or around the southwest margin of the forebulge into the back-bulge region. Initial deposition of the Morrison Formation (Windy Hill, Tidwell, and Salt Wash Members) occurred as a result of eastward progradation of marginal and nonmarine depositional systems into the back-bulge depozone during Oxfordian retreat of the Sundance–Stump sea.

Late Oxfordian–Kimmeridgian deposition of the lower Morrison Formation was followed by early Tithonian deposition of upper Salt Wash Member sandstones and conglomerates (Fig. 13A). This deposition was associated with the progradation of coarse-grained fluvial facies from the thrust belt to the west. Following Salt Wash deposition, lower Brushy Basin Member fluvial systems underwent a transition from braided to meandering channel morphologies. This change may have been associated with the influx of abundant fine-grained material in the form of volcanic air-fall (Currie 1997a). The end result of this transition was the establishment of Brushy Basin laterally stable, low-sinuosity fluvial systems during late Tithonian to early Neocomian time. Depositional filling of the Late Jurassic–Early Cretaceous back-bulge depozone produced west-directed onlap of the forebulge located in central Utah (Fig 12B; Currie 1994).

Insofar as the amount of flexural subsidence in the back-bulge region predicted by flexural models is very low (< 20 m for normal crustal rigidities), deposition of the Morrison Formation above the forebulge and back-bulge depozones may have been enhanced by dynamic subsidence (Lawton 1994; DeCelles and Currie 1996). A cessation of regional dynamic subsidence during the Neocomian may have resulted in a decrease in back-bulge accommodation and incision and deposition of the Buckhorn Conglomerate (Fig. 13C).

Following deposition of the Buckhorn Conglomerate, eastward propagation of thrust loads in the Sevier belt resulted in foredeep flexural subsidence in areas of central Utah previously occupied by the Late Jurassic forebulge. Foredeep development in central Utah was accompanied by migration of the forebulge into eastern Utah and western Colorado (Currie 1994). During that time, underfilling of the foredeep cut off sediment supply to areas uplifted by the forebulge. The resulting unconformity allowed thick calcrete deposits to form on the filled Buck-

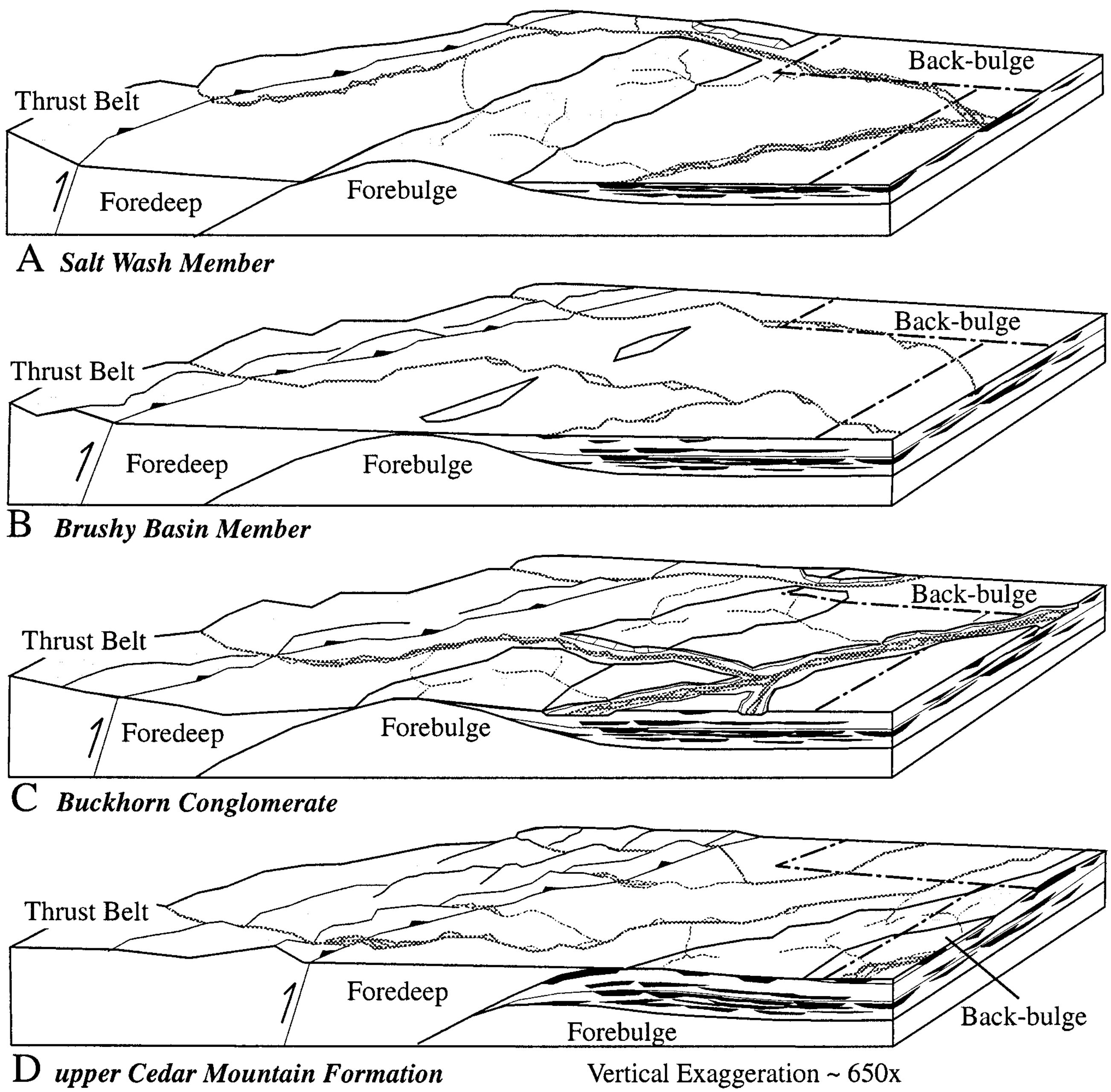

FIG. 13.—Schematic block diagrams showing the evolution of the Late Jurassic–Early Cretaceous foreland-basin system in Utah and western Colorado. Cross-section views of the back-bulge depozone depict generalized stratigraphic relationships and fluvial-channel architecture. **A)** Kimmeridgian–Tithonian deposition of the Salt Wash Member; **B)** Late Tithonian deposition of the Brushy Basin Member; **C)** Mid-Neocomian deposition of the Buckhorn Conglomerate; **D)** Aptian–Albian deposition of the upper Cedar Mountain Formation. Shaded areas represent uplifted areas on the forebulge and in the thrust belt. Dashed line shows approximate position of present-day Utah, Wyoming, and Colorado state lines.

horn valley surface and above previously exposed areas adjacent to the valley margins. Subsequent overfilling of the foredeep during Aptian–Albian time resulted in depositional onlap of Cedar Mountain fluvial systems onto the forebulge depozone in eastern Utah and western Colorado (Fig. 13D).

The possible presence of a flexural forebulge in central Utah during the Late Jurassic implies the existence of a flexural foredeep in west-central Utah during the Late Jurassic. Although no Upper Jurassic foredeep deposits are preserved in west-central Utah, structural reconstructions of the Sevier belt indicate that $>$ 4 km of Upper Jurassic–Lower Cretaceous sediment could have been eroded from this area as a result of Late Cretaceous thrust-related uplift (Royse 1993). Active Late Jurassic thrusting in the central Cordillera is supported by reconstructions of the Canyon Range thrust sheet that indicate $>$ 40 km of pre-Aptian displacement in west central Utah, as well as pre-140 Ma emplacement of thrust terranes in northern Utah (Currie 1997b; Camilleri et. al 1997) Active Late Jurassic thrusting in the Sevier belt to the south is also supported by isotopic dating of dikes that crosscut the Clark Mountain thrust system in southern Nevada and southeastern California that indicated a 144 Ma age of thrusting (Walker et al. 1995).

CONCLUSIONS

On the basis of isotopic and palynologic dating of rocks in the study area and regional lithostratigraphic and chronostratigraphic correlations, the Morrison Formation was deposited between Oxfordian and Tithonian time, although deposition may have extended into the Early Cretaceous. Similar correlations indicate that the upper Cedar Mountain Formation was deposited during late Neocomian–Albian time. Although the age of the Buckhorn Conglomerate Member is unknown, the ages of bounding units suggest deposition during mid-Neocomian time.

The lower Morrison Formation consists of marginal and nonmarine facies that were deposited during Oxfordian–Kimmeridgian retreat of shallow marine deposystems. Upper parts of the Morrison are entirely nonmarine and contain braided, meandering, and laterally stable, low-sinuosity fluvial facies, as well as lacustrine deposits. The Cedar Mountain Formation contains gravelly braided fluvial facies of the Buckhorn Conglomerate that are overlain by laterally stable, low-sinuosity fluvial channels and associated overbank and lacustrine facies.

Morrison and Cedar Mountain sandstones contain quartz, feldspar, chert, and volcanic lithic grains. Paleocurrent and petrologic data indicate that sources for these sandstones were lower Mesozoic, Paleozoic, and Proterozoic sedimentary rocks of the Cordillera west of the study area. The progressive unroofing of the source area indicated by Morrison and Cedar Mountain sandstone compositions indicate that Cordilleran thrusting was active throughout Late Jurassic and Early Cretaceous time.

Deposition of the Morrison and Cedar Mountain Formations in the study area was related to interactions between basin accommodation development, sediment supply, and migration of foreland-basin system flexural components during the Late Jurassic and Early Cretaceous. The Morrison Formation and Buckhorn Conglomerate were deposited in a back-bulge setting east of a flexural forebulge in central Utah. The unconformity represented by the calcrete zone at the base of the upper Cedar Mountain Formation formed as a result of forebulge migration into eastern Utah during the Early Cretaceous. Deposition of the upper Cedar Mountain in the study area occurred as the Early Cretaceous foredeep became overfilled and onlapped the uplifted forebulge.

ACKNOWLEDGMENTS

This study was partly supported by National Science Foundation grant EAR-9205382, and summer research grants from the Colorado Scientific Society, the Geological Society of America, and Sigma Xi. I thank field assistants K.C. Pankow, B.D. Ritts, J.A. Trop, and R.R. Rasmussen for their help in gathering data. Special thanks go to C.E. Turner and F. Peterson for helping me get started and for sharing their vast knowledge of the Morrison. A debt of gratitude goes to D.J. Chure and the staff at Dinosaur National Monument for their hospitality, T.M. Demko for his informative insight on the Morrison, and J.C. Coogan for, among other things, access to his Sevier belt cross sections. I am grateful to P.G. DeCelles for the hours of informative discussion and the informal reviews of the manuscript. Reviews by T.F. Lawton, W.M. Aubrey, K.D. Ridgway, K.A. Giles, and B.D. Ricketts greatly improved the quality of this paper. Above all, I would like to thank R.K. Schwartz, whose encouragement and assistance helped make this investigation possible.

REFERENCES

Allmendinger, R.W., 1983, Geologic map of the North Hansel Mountains, Idaho and Utah: U.S. Geological Survey, Miscellaneous Field Studies Map MF-1643.

Arakel, A.V., 1986, Evolution of calcrete in paleodrainages of the Lake Napperby Area, central Australia: Palaeogeography, Palaeoclimatology, Palaeoecology, v. 54. p. 283–303.

Armstrong, F.C., and Cressman, E.R., 1963, The Bannock thrust zone, southeastern Idaho: U.S. Geological Survey, Professional Paper 374-J, 22 p.

Bell, T.E., 1986, Deposition and diagenesis of the Brushy Basin Member and upper part of the Westwater Canyon Member of the Morrison Formation, San Juan Basin, New Mexico, *in* Turner-Peterson, C.E., Santos, E.S., and Fishman, N.S., eds., A Basin Analysis Case Study: The Morrison Formation Grants Uranium Region New Mexico: American Association of Petroleum Geologists, Studies in Geology 22, p. 1847–1866.

Bjerrum, C.J., and Dorsey, R.J., 1995, Tectonic controls on deposition of Middle Jurassic strata in a retroarc foreland basin, Utah–Idaho trough, western interior, United States: Tectonics, v. 14, p. 962–978.

Camilleri, P, Yonkee, A., Coogan, J., DeCelles, P., McGrew, A., and Wells, M., 1997, Hinterland to foreland transect through the Sevier orogen, northeast Nevada to north central Utah: structural style, metamorphism, and kinematic history of a large contractional orogenic wedge, *in* Link, P.L., and Kowallis, B.J., eds., Proterozoic to Recent Stratigraphy, Tectonics, and Volcanology, Utah, Nevada, Southern Idaho, and Central Mexico: Brigham Young University, Geology Studies, no. 42, part I, p. 297–380.

Cifelli, R.L., Kirkland, J.I., Weil, A., Deino, A.L., and Kowallis, B.J., 1997, High precision $^{40}Ar/^{39}Ar$ geochronology and the advent of North America's Late Cretaceous terrestrial fauna: National Academy of Science, Proceedings, v. 94, p. 11,163–11,167.

Clifton, H.E., 1969, Beach lamination: nature and origin: Marine Geology, v. 7, p. 553–559.

Coogan, J.C., 1992, Thrust systems and displacement transfer in the Wyoming–Idaho–Utah thrust belt [unpublished Ph.D. thesis]: Laramie, Wyoming, University of Wyoming, 239 p.

Currie, B.S., 1994, ''Back-bulge'' to foredeep evolution of the Late Jurassic–Early Cretaceous Cordilleran foreland basin: Evidence from the Morrison and Cedar Mountain Formations, central-eastern Utah (abstract): Geological Society of America, Abstracts with Programs, v. 26, no. 6, p. 9.

Currie, B.S., 1995, Configuration of the Early Cretaceous Cordilleran foreland basin system, Utah and Colorado (abstract): Geological Society of America, Abstracts with Programs, v. 27, no. 4, p. 7.

Currie, B.S., 1997a, Sequence stratigraphy of nonmarine Jurassic–Cretaceous rocks, central Cordilleran foreland-basin system: Geological Society of America, Bulletin, v. 109, p. 1206–1222.

Currie, 1997b, Jurassic–Cretaceous evolution of the central Cordilleran foreland-basin system [unpublished Ph.D. thesis]: Tucson, Arizona, University of Arizona, 239 p.

Currie, B.S., Pankow, K.C., and Ritts, B.D., 1993, Depositional architecture and sequence stratigraphy of the mid-Cretaceous Dakota Formation, NE Utah–NW Colorado (abstract): Geological Society of America, Abstracts with Programs, v. 25, no. 5, p. 26.

DeCelles, P.G., and Burden, E.T., 1992, Nonmarine sedimentation in the overfilled part of the Jurassic–Cretaceous Cordilleran foreland basin: Morrison and Cloverly Formations, central Wyoming, USA: Basin Research, v. 4, p 291–313.

DeCelles, P.G., and Currie, B.S., 1996, Long-term sediment accumulation in the Middle Jurassic–early Eocene Cordilleran retroarc foreland-basin system: Geology, v. 24, p. 591–594.

DeCelles, P.G., and Giles, K.G., 1996, Foreland-basin systems: Basin Research, v. 8, p. 105–123.

DeCelles, P.G., Langford, R.P., and Schwartz, R.K., 1983, Two new methods of paleocurrent determination from trough cross-stratification: Journal of Sedimentary Petrology, v. 53, p. 629–642.

DeCelles, P.G., Lawton, T.F., and Mitra, G., 1995, Thrust timing, growth of structural culminations, and synorogenic sedimentation in the type area of the Sevier orogenic belt, western United States: Geology, v. 23, p. 699–702.

DeCelles, P.G., Pile, H.T., and Coogan, J.C., 1993, Kinematic history of the Meade thrust based on provenance of the Bechler Conglomerate at Red Mountain, Idaho, Sevier thrust belt: Tectonics, v. 12, p. 1436–1450.

DeCelles, P.G., Pile, H.T., and Currie, B.S., 1992, Regional stratigraphic analysis of Jurassic–Cretaceous nonmarine rocks, central western interior basin (abstract): SEPM 1992 Theme Meeting, Mesozoic of the Western Interior, Ft. Collins, Colorado, p. 23.

Demko, T.M., Currie, B.S., and Nicoll, K.A., 1996, Paleosols at sequence boundaries in the Upper Jurassic Morrison Formation, Colorado Plateau and Rocky Mountain Regions, USA (abstract): Geological Society of America, Abstracts with Programs, v. 28, no. 7.

Dickinson, W.R., and Snyder, W.S., 1978, Plate tectonics of the Laramide orogeny, *in* Matthews, V., ed., Laramide Folding Associated with Block Faulting in the Western United States: Geological Society of America, Memoir 151, p. 355–366.

Dickinson, W.R., Beard, L.S., Brakenridge, G.R., Erjavec, J.L., Ferguson, R.C., Inman, K.F., Knepp, R.A., Lindberg, F.A., and Ryberg, P.T., 1983, Provenance of North American Phanerozoic sandstones in relationship to tectonic setting: Geological Society of America, Bulletin, v. 94, p. 222–235.

Furer, L.C., 1970, Petrology and stratigraphy of nonmarine Upper Jurassic–Lower Cretaceous rocks of western Wyoming and southeastern Idaho: American Association of Petroleum Geologists, Bulletin, v. 54, p. 2285–2302.

Ginsburg, R.N., 1975, Tidal Deposits: A Casebook of Recent Examples and Fossil Counterparts: New York, Springer-Verlag, 428 p.

Gradstein, F.M., Agterberg, F.P., Ogg, J.G., Hardenbol, J., Van Veen, P., Thierry, J., and Huang, Z., 1995, A Triassic, Jurassic and Cretaceous time scale, *in* Berggren, W.A., Kent, D.V., Aubry, M.P., and Hardenbol, J., eds., Geochronology, Time Scales and Global Stratigraphic Correlation: SEPM, Special Publication 54, p. 95–125.

Gurnis, M., 1992, Rapid continental subsidence following initiation and evolution of subduction: Science, v. 255, p. 1556–1558.

Hansen, W.R., 1965, Geology of the Flaming Gorge area Utah–Colorado–Wyoming: U.S. Geological Survey, Professional Paper 490, 196 p.

Heller, P.L., and Paola, C., 1989, The paradox of Lower Cretaceous gravels and the initiation of thrusting in the Sevier orogenic belt, United States western interior: Geological Society of America, Bulletin, v. 101, p. 864–975.

Heller, P.L., Bowdler, S.S., Chambers, H.P., Coogan, J.C., Hagen, E.S., Shuster, M.W., Winslow, N.S., and Lawton, T.F., 1986, Timing and initial thrusting in the Sevier orogenic belt, Idaho–Wyoming and Utah: Geology, v. 14, p. 388–391.

Hintze, L.F., 1988, Geological history of Utah, *in* Kowallis, B.J., ed., Brigham Young University, Geology Studies, Special Publication 7, 202 p.

Hudec, M.R., 1992, Mesozoic structural and metamorphic history of the central Ruby Mountains metamorphic core complex, Nevada: Geological Society of America, Bulletin, v. 104, p. 1086–1100.

HUNTER, R.E., 1977, Basic types of stratification in small eolian dunes: Sedimentology, v. 24, p. 361–387.

HUNTER, R.E., CLIFTON, H.E., AND PHILLIPS, R.L., 1979, Depositional processes, sedimentary structures, and predicted vertical sequences in barred nearshore systems, southern Oregon coast: Journal of Sedimentary Petrology, v. 49, p. 711–726.

INGERSOLL, R.V., BULLARD, T.F., FORD, R.L., GRIMM, J.P., PICKLE, J.D., AND SARES, S.W., 1984, The effect of grain size on detrital modes: a test of the Gazzi–Dickinson point-counting method: Journal of Sedimentary Petrology, v. 54, p. 103–116.

JORDAN, T.E. 1981, Thrust loads and foreland basin evolution, Cretaceous, western United States: American Association of Petroleum Geologists, Bulletin, v. 43, p. 2167–2196.

KATICH, P.J., 1951, Recent evidence of lower Cretaceous deposits in the Colorado Plateau: American Association of Petroleum Geologists, Bulletin, v. 35, p. 2093–2094.

KHALAF, F.I., 1990, Occurrence of phretic dolocrete within Tertiary clastic deposits of Kuwait, Arabian Gulf: Sedimentary Geology, v. 80, p. 223–239.

KIRKLAND, J.I., 1992, Dinosaurs define a two-fold Lower Cretaceous zonation of the Cedar Mountain Formation, central Utah (abstract): Geological Society of America, Abstracts with Programs, v. 24, p. 22.

KIRKWOOD, S.G., 1976, Stratigraphy and petroleum potential of the Cedar Mountain and Dakota Formations, northwestern Colorado [unpublished M.S. thesis]: Golden, Colorado, Colorado School of Mines, 193 p.

KOWALLIS, B.J., CHRISTIANSEN, E.H., AND DEINO, A.L., 1991, Age of the Brushy Basin Member of the Morrison Formation, Colorado Plateau, western USA: Cretaceous Research, v. 12, 483–493.

KOWALLIS, B.J., CHRISTIANSEN, E.H., DEINO, A.L., PETERSON, F., TURNER, C.E., KUNK, M.J., AND OBRADOVICH, J.D., 1998, The age of the Morrison Formation: Modern Geology, in press.

LAWTON, T.F., 1994, Tectonic setting of Mesozoic sedimentary basins, Rocky Mountain region, United States, *in* Caputo, M.V., Peterson, J.A., and Franczyk, K.J., eds., Mesozoic Systems of the Rocky Mountain region, USA: SEPM, Rocky Mountain Section, Denver, Colorado, p. 1–25.

MACHETTE, M.N., 1985, Calcic soils of the southwestern United States, *in* Weide, D.L., and Faber, M.L., eds., Soils and Quaternary Geology of the Southwestern United States: Geological Society of America, Special Paper 203, p. 1–21.

MACK, G.H., 1992, Paleosols as an indicator of climate change at the Early–Late Cretaceous boundary, southwestern New Mexico: Journal of Sedimentary Petrology, v. 62, p. 483–94.

MANSFIELD, G.R., 1927, Geography, geology, and mineral resources of a part of southeastern Idaho: U.S. Geological Survey, Professional Paper 152, 409 p.

MIALL, A.D., 1977, A review of the braided river depositional environment: Earth-Science Reviews, v. 13, p. 1–62.

MILLER, D.M., 1992, Mesozoic tectonics of northwestern Utah and adjacent Nevada (abstract): Geological Society of America, Abstracts with Programs, v. 26, no. 6, p. 53.

MITROVICA, A.X., BEAUMONT, C., AND JARVIS, G.T., 1989, Tilting of continental interiors by the dynamic effects of subduction: Tectonics, v. 8, p. 1079–1094.

MOLENAAR, C.M., AND COBBAN, W.A., 1991, Middle Cretaceous stratigraphy on the south and east sides of the Uinta basin, northeastern Utah and northwestern Colorado: U.S. Geological Survey, Bulletin 1787-P, 34 p.

PETERSON, F., 1987, The search for the source area of Morrison (Upper Jurassic) clastics on the Colorado Plateau (abstract): Geological Society of America, Abstracts with Programs, v. 19, p. 804.

PETERSON, F., 1988, Stratigraphy and Nomenclature of Middle and Upper Jurassic Rocks, Western Colorado Plateau, Utah and Arizona: U.S. Geological Survey, Bulletin 1633-B, 37 p.

PETERSON, F., 1992, Chronology of the Jurassic system in the western interior basin (abstract): SEPM Theme Meeting, Mesozoic of the Western Interior, Fort Collins, Colorado, p. 53.

PETERSON, F., 1994, Sand dunes, sabkhas, streams, and shallow streams: Jurassic paleogeography in the southern part of the western interior basin, *in* Caputo, M.V., Peterson, J.A., and Franczyk, K.J., eds., Mesozoic Systems of the Rocky Mountain region, USA: SEPM, Rocky Mountain Section, Denver, Colorado, p. 233–272.

PIPIRINGOS, G.N., AND O'SULLIVAN, R.B., 1978, Principal unconformities in Triassic and Jurassic rocks, western interior United States—A preliminary survey: U.S. Geological Survey, Professional Paper 1035-A, 29 p.

RAMOS, A., AND SOPEÑA, A., 1983, Gravel bars in low sinuosity streams (Permian and Triassic, central Spain), *in* Collinson, J.D., and Lewin, J., eds., Modern and Ancient Fluvial Systems: International Association of Sedimentologists, Special Publication 6, p. 301–312.

REINECK, H.E., AND WUNDERLICH, F., 1968, Classification and origin of flaser and lenticular bedding: Sedimentology, v. 11, p. 99–104.

ROYSE, F., 1993, Case of the phantom foredeep: Early Cretaceous in west-central Utah: Geology, v. 21, p. 133–136.

ROYSE, F., WARNER, M.A., AND REESE, D.L., 1975, Thrust-belt structural geometry and related stratigraphic problems, Wyoming–Idaho–northern Utah, *in* Bolyard, D.W., ed., Symposium on Deep Drilling Frontiers of the Central Rocky Mountains: Rocky Mountain Association of Geologists, Denver, Colorado, p. 41–54.

RUST, B.R., 1972, Structure and process in a braided river: Sedimentology, v. 18, p. 221–245.

RUST, B.R., 1978, Depositional models for braided alluvium, *in* Miall, A.D., ed., Fluvial Sedimentology: Canadian Society of Petroleum Geologists, Memoir 5, p. 605–625.

RUST, B.R., 1981, Sedimentation in an arid-zone anastomosing fluvial system: Cooper's Creek, central Australia: Journal of Sedimentary Petrology, v. 51, p. 745–755.

SCHUDACK, M.E., TURNER, C.E., AND PETERSON, F., 1998, Biostratigraphy, paleoecology, and biology of charophytes and ostracodes from the Upper Jurassic Morrison Formation, Western Interior, U.S.A.: Modern Geology, in press.

SCHUMANN, R.R., 1989, Morphology of Red Creek, Wyoming, an arid-region anastomosing channel system: Earth Surface Processes and Landforms, v. 14, p. 277–288.

SCHWANS, P., 1988, Depositional response of the Pigeon Creek Formation, Utah to initial fold–thrust deformation in a differentially subsiding foreland basin, *in* Schmidt, C.J., and Perry, W.J., eds., Interaction of the Rocky Mountain Foreland and the Cordilleran Thrust Belt: Geological Society of America, Memoir 171, p. 531–556.

SHANLEY, K.W., AND MCCABE, P.J, 1994, Perspectives on the sequence stratigraphy of continental strata: American Association of Petroleum Geologists, Bulletin, v. 78, p. 544–568.

SHANMUGAM, G., 1988, Origin, recognition and importance of erosional unconformities in sedimentary basins, *in* Kleinspehn, K.L., and Paola, C., eds, New Perspectives in Basin Analysis: New York, Springer-Verlag, p. 83–108.

SHANMUGAM, G., AND HIGGINS, J.B., 1988, Porosity enhancement from chert dissolution beneath Neocomian unconformity: Ivishak Formation, North Slope, Alaska: American Association of Petroleum Geologists, Bulletin, v. 72, p. 523–535.

SIMMONS, G.C., 1957, Contact of the Burro Canyon Formation with the Dakota Sandstone, Slick Rock district: American Association of Petroleum Geologists, Bulletin, v. 41, p. 2519–2529.

SIPPEL, K.N., 1982, Depositional and tectonic setting of the Ephraim Formation, southeast Idaho–Western Wyoming [unpublished M.S. thesis]: Laramie, Wyoming, University of Wyoming, 157 p.

SMITH, N.D., AND PÉREZ-ARLUCEA, M., 1994, Fine-grained splay deposition in the avulsion belt of the lower Saskatchewan River, Canada: Journal of Sedimentary Research, v. B64, p. 159–168.

SNOKE, A.W., WRIGHT, J.E., HUDEC, M.R., AND MCGREW, A.J., 1992, Mesozoic magmatic–metamorphic deformational history of the Ruby Mountains–East Humbolt Range, Nevada (abstract): Geological Society of America, Abstracts with Programs, v. 26, no. 6, p. 63.

SPÖTL, C., AND WRIGHT, V.P., 1992, Groundwater dolocretes from the Upper Triassic Paris basin, France: a case study of an arid, continental diagenetic facies: Sedimentology, v. 39, p. 1119–1136.

SPRINKEL, D.A., WEISS, M.P., FLEMING, R.W., AND WAANDERS, G.L., 1998, Redefining the Lower Cretaceous stratigraphy of central Utah and an example of the structural development with the foreland basin, *in* Lageson, D.A., and Schmitt, J.A., eds., Recent Advances in Understanding the Sevier Orogenic Belt of the Western United States: Geological Society of America, Special Paper, in press.

STOKES, W.L., 1944, Morrison and related deposits in and adjacent to the Colorado Plateau: Geological Society of America, Bulletin, v. 41, p. 951–992.

STOKES, W.L., 1952, Lower Cretaceous in the Colorado Plateau: American Association of Petroleum Geologists, Bulletin, v. 36, p. 1766–1776.

STOKES, W.L., 1972, Stratigraphic problems of the Triassic and Jurassic sedimentary rocks of central Utah, *in* Baer, J.L., and Callaghan, E., eds., Plateau–Basin and Range Transition Zone, Central Utah: Utah Geological Association, Publication 2, p. 21–28.

SUTTNER, L.J., 1969, Stratigraphic and petrologic analysis of Upper Jurassic–Lower Cretaceous Morrison and Kootenai Formations, southwest Montana: American Association of Petroleum Geologists, Bulletin, v. 53, p. 1391–1410.

THAYN, G.F., 1973, Three species of petrified dicotylededonous wood from the Lower Cretaceous Cedar Mountain Formation of Utah [unpublished M.S. thesis]: Provo, Utah, Brigham Young University, 43 p.

THORMAN, C.H., KETNER, K.B., AND PETERSON, F., 1992, The Middle to Late Jurassic Elko orogeny in eastern Nevada and western Utah (abstract): Geological Society of America, Abstracts with Programs, v. 26, no. 6, p. 66.

TSCHUDY, R.H., TSCHUDY, B.D., AND CRAIG, L.C., 1984, Palynological evaluation of the Cedar Mountain and Burro Canyon Formations, Colorado Plateau: U.S. Geological Survey, Professional Paper 1281, 24 p.

TURNER, C.E., 1992, Study of the Jurassic Morrison Formation at Dinosaur National Monument, Colorado and Utah (abstract): SEPM Theme Meeting; Mesozoic of the Western Interior, Fort Collins, Colorado, p. 64.

TURNER, C.E., AND FISHMAN, N.S., 1991, Jurassic Lake T'oo'dichi': A large alkaline, saline lake, Morrison Formation, eastern Colorado Plateau: Geological Society of America, Bulletin, v. 103, p. 538–558.

VAUGHN, R.L., AND PICARD, M.D., 1976, Stratigraphy, Sedimentology, and Petroleum Potential of Dakota Formation, Northeastern Utah: Uinta Basin, Rocky Mountain Association of Geologists Guidebook, p. 267–279.

WALKER, J.D., BURCHFIEL, B.C., AND DAVIS, G.A., 1995, New age controls on the initiation of foreland belt thrusting in the Clark Mountains, southern California: Geological Society of America, Bulletin, v. 107, p. 742–750.

WARD, L.G., AND ASHLEY, G.M., 1989, Physical processes and sedimentology of siliciclastic-dominated lagoonal systems: Marine Geology, v. 88, p. 181–364.

WEIMER, R.J., HOWARD, J.D., AND LINDSAY, D.R., 1982, Tidal flats and associated tidal channels, *in* Scholle, P.A., and Spearing, D., eds., Sandstone Depositional Environments: American Association of Petroleum Geologists, Memoir 31, p. 191–245.

WEISS, M.P., AND ROCHE, M.G., 1988, The Cedar Mountain Formation (Lower Cretaceous) in the Gunnison Plateau, central Utah, *in* Schmidt, C.J., and Perry, W.J., eds., Interaction of the Rocky Mountain Foreland and the Cordilleran Thrust Belt: Geological Society of America, Memoir 171, p. 557–569.

WELLS, M.L., 1992, Mesozoic and Cenozoic (?) deformation in the Black Pine and Raft River Mountains, southern Idaho and northwestern Utah (abstract): Geological Society of America, Abstracts with Programs, v. 26, no. 6, p. 68.

WILLIAMS, P.F., AND RUST, B.R., 1969, The sedimentology of a braided river: Journal of Sedimentary Petrology, v. 39, p. 649–679.

WILLIS, G.C., 1986, Geologic map of the Salina quadrangle, Sevier County, Utah: Utah Geological and Mineral Survey, Map 83, 20 p., scale 1:24,000.

WILTSCHKO, D.W., AND DORR, J.A., JR., 1983, Timing of deformation in the overthrust belt and foreland of Idaho, Wyoming, and Utah: American Association of Petroleum Geologists, Bulletin, v. 68, p. 156–194.

YINGLING, V.L., 1987, Timing of initiation of the Sevier orogeny: Morrison and Cedar Mountain

Formations and Dakota Sandstone, east-central Utah [unpublished M.S. thesis]: Laramie, Wyoming, University of Wyoming, 169 p.
YINGLING, V.L., AND HELLER, P.L., 1992, Timing and record of foreland sedimentation during the initiation of Sevier orogenic belt in central Utah: Basin Research, v. 4, p. 279–290.
YONKEE, W.A., 1990, Geometry and mechanics of basement and cover deformation, Farmington Canyon complex, Sevier orogenic belt, Utah [unpublished Ph.D. thesis]: Salt Lake City Utah, University of Utah, 255 p.
YONKEE, W.A., 1992, Basement–cover relations, Sevier orogenic belt: Geological Society of America, Bulletin, v. 104, p. 280–302.
YOUNG, R.G., 1970, Lower Cretaceous of Wyoming and the southern Rockies: The Mountain Geologist, v. 7, no. 3, p. 105–121.

Received 8 July 1997; accepted 19 February 1998.

APPENDIX 1.—*Utah-Colorado measured stratigraphic section locations.*

Abbreviation	Section	Location	
Figure 3			
1FD	1 Finch Draw	sec. 21, 26, T. 3 N, R. 20 E	Daggett Co., UT
1SC	1 Steinaker Canal	sec. 2, T. 3 S, R. 22 E	Uintah Co., UT
1RF	1 Red Fleet	sec. 2, T. 3 S, R. 22 E	Uintah Co., UT
1SMA	1 Split Mountain Anticline	sec. 18, T. 4 S, R. 23 E	Uintah Co., UT
2IP	2 Island Park Road	sec. 5, 6, T. 4 S, R. 23 E	Uintah Co., UT
1OD	1 Orchid Draw	sec. 22, 27, T. 4 S, R. 23 E	Uintah Co., UT
1TD	1 Theropod Draw	sec. 26, T. 4 S, R. 23 E	Uintah Co., UT
1IP	1 Island Park Rd	sec. 4, T. 4 S, R. 24 E	Uintah Co., UT
TCW	Trail Creek West	sec. 34, 10, T. 5 N, R. 23 E	Uintah Co., UT
1BC	1 Bull Canyon	sec. 29, T. 4 N, R. 104 W	Moffat Co., CO
1MHQ	1 Monument Headquarters	sec. 8, T. 3 N, R. 103 W	Moffat Co., CO
RWD	Rock Wall Draw	sec. 5, T. 3 N, R. 101 W	Moffat Co., CO
1IC	1 Irish Canyon	sec. 11, T. 10 N, R. 101 W	Moffat Co., CO
LHD	Left-Hand Draw	sec. 35, T. 9 N, R. 100 W	Moffat Co., CO
1DP	1 Deerlodge Park	sc. 28, T. 6 N, R. 99 W	Moffat Co., CO
Figure 10			
	Baker Ranch	sec. 18, T. 26 S, R. 4 E	Sevier Co., UT
	Last Chance Wash	sec. 7, T. 25 S, R. 6 E	Emery Co., UT
	I-70	sec. 7–8, T. 23 S, R 7 E	Emery Co., UT
	San Rafael River	sec. 22–27, T. 19 S, R. 9 E	Emery Co., UT
	Cedar Mountain	sec. 33, T. 18 S, R. 10 E	Emery Co., UT
	Green River Cut-Off	sec. 5, T. 19 S, R, 14 E	Emery Co., UT